ADVANCED MATERIALS
www.advmat.de

Anisotropic Microcarriers: Fabrication Strategies and Biomedical Applications

Yingying Hou, Leyan Xuan, Weihong Mo, Ting Xie, Juan Antonio Robledo Lara, Jialin Wu, Junjie Cai, Farzana Nazir, Long Chen, Xin Yi, Sifan Bo, Huaibin Wang, Yuanye Dang, Maobin Xie,* and Guosheng Tang**

Anisotropic microcarriers (AMs) have attracted increasing attention. Although significant efforts have been made to explore AMs with various morphologies, their full potential is yet to be realized, as most studies have primarily focused on materials or fabrication methods. A thorough analysis of the interactional and interdependent relationships between these factors is required, along with proposed countermeasures tailored for researchers from various backgrounds. These countermeasures include specific fabrication strategies for various morphologies and guidelines for selecting the most suitable AM for certain biomedical applications. In this review, a comprehensive summary of AMs, ranging from their fabrication methods to biomedical applications, based on the past two decades of research, is provided. The fabrication of various morphologies is investigated using different strategies and their corresponding biomedical applications. By systematically examining these morphology-dependent effects, a better utilization of AMs with diverse morphologies can be achieved and clear strategies for breakthroughs in the biomedical field are established. Additionally, certain challenges are identified, new frontiers are opened, and promising and exciting opportunities are provided for fabricating functional AMs with broad implications across various fields that must be addressed in biomaterials and biotechnology.

1. Introduction

The history of microparticles (from 1 to 1000 µm) dates back to the 1960s. These particles are applicable in diverse fields, including biotechnology, chemistry, and materials science.[1] As research on microparticles advanced within the scientific community, Janus particles, similar to the Chinese "Yinyang" or Roman Janus, were proposed to consist of two compartments with distinct chemical or physical properties.[2] Among the pioneers that recognized the potential and significance of Janus particles was Nobel Laureate P. G. de Gennes, who discussed these particles in his Nobel lecture, "Soft Matter," in 1991.[3] Since then, research on Janus particles has significantly expanded, transcending the traditional domains of colloids and soft matter. A growing variety of synthetic strategies for Janus particles has facilitated this rapid development. Furthermore, certain prerequisites exist for complex applications along with the advancement of diverse research methods. A new concept has also been proposed, i.e., multicompartmental microparticles or microfibers, collectively referred to as anisotropic microcarriers (AMs). AMs can be engineered by integrating multifunctional building blocks with distinct magnetic, electrical, optical, or chemical properties. The anisotropy from the heterogeneous structure offers unique material functionalities and surface chemistry that are difficult to attain with

Y. Hou, L. Xuan, W. Mo, T. Xie, J. Wu, J. Cai, F. Nazir, L. Chen, S. Bo, H. Wang, Y. Dang, G. Tang
Guangzhou Municipal and Guangdong Provincial Key Laboratory of Molecular Target and Clinical Pharmacology
the NMPA and State Key Laboratory of Respiratory Disease
School of Pharmaceutical Sciences and the Fifth Affiliated Hospital
Guangzhou Medical University
Guangzhou 511436, P. R. China
E-mail: dangyuanye@gzhmu.edu.cn; guoshengtang@gzhmu.edu.cn

J. A. R. Lara
Division of Engineering in Medicine
Department of Medicine
Brigham and Women's Hospital
Harvard Medical School
Cambridge, MA 02139, USA

X. Yi
Key Laboratory of Bioactive Materials
Ministry of Education
College of Life Sciences
Nankai University
Weijin Road 94, Tianjin 300071, P. R. China

Y. Hou, L. Chen, M. Xie
The Fourth Affiliated Hospital of Guangzhou Medical University
School of Biomedical Engineering
Guangzhou Medical University
Guangzhou 511436, P. R. China
E-mail: maobinxie@gzhmu.edu.cn

The ORCID identification number(s) for the author(s) of this article can be found under https://doi.org/10.1002/adma.202416862

DOI: 10.1002/adma.202416862

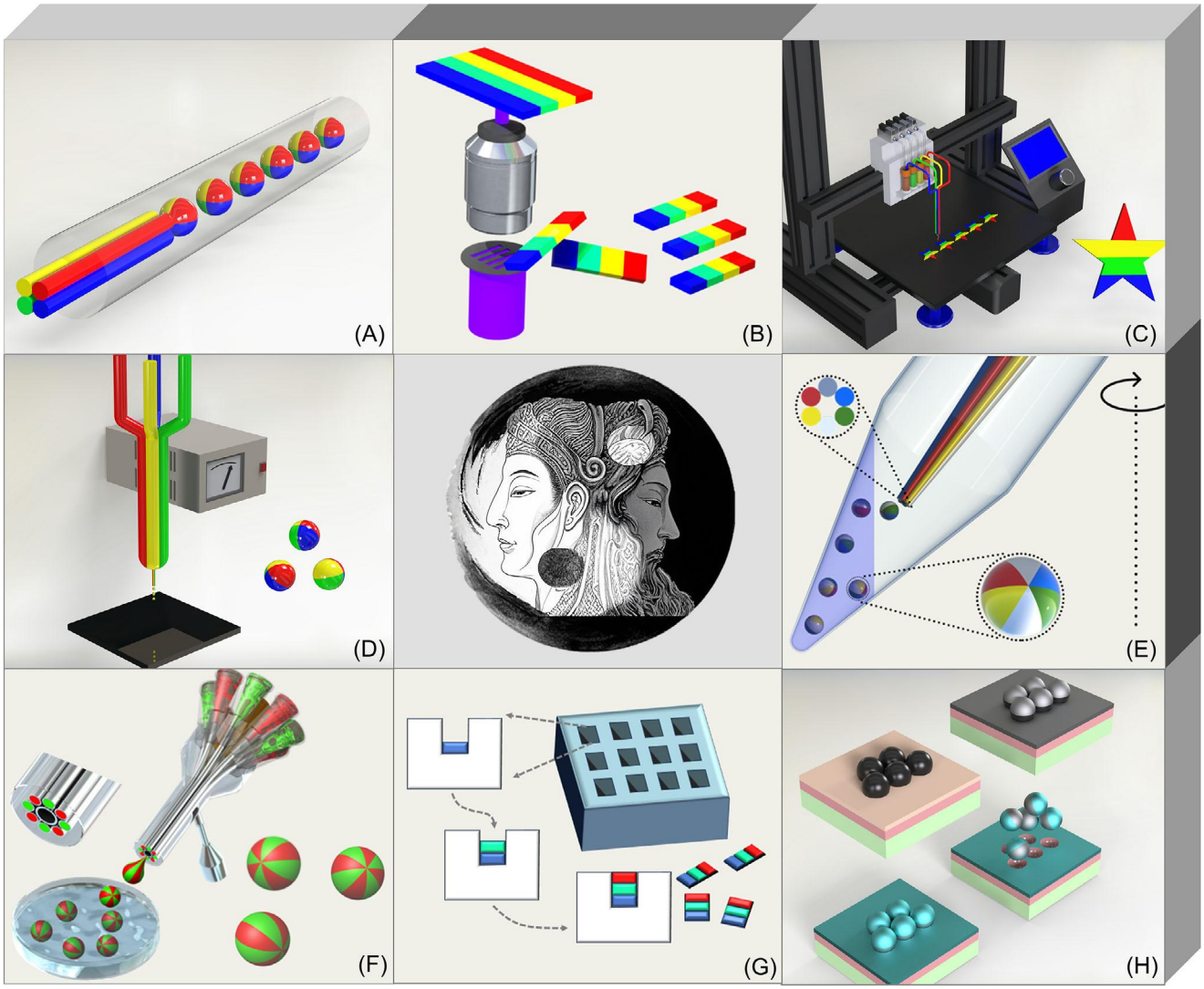

Figure 1. Schematics of fabrication of anisotropic microcarriers with a series of methods including A) microfluidics, B) lithography, C) 3D printing, D) EHD cojetting, E) centrifugation method, F) gas-based method, G) template method, and H) sputter coating method.

single-compartment particles, thereby creating novel opportunities across a range of application domains (Table S1, Supporting Information).

In recent decades, considerable interest in AMs that showed potential for "intelligent" applications in the field of biomedicine has existed. Numerous reviews have been published on the applications of nano- and micrometer-sized particles. However, these studies have primarily focused on homogenous or Janus microparticles.[4] Only a few reviews have addressed multicompartmental microparticles. Among them, most have focused on microfluidic strategies and overlooked other advanced methods. Notably, comprehensive reviews on AMs are currently lacking, particularly those emphasizing multicompartmental microcarriers, including particles, fibers, and extrasize patterns. Enhancing our understanding of AMs and broadening their potential use across various research fields, particularly biomedical applications, requires a thorough examination and summary of recent studies. To date, several approaches have been developed to address the challenges of AM fabrication, including microfluidics,[5] lithography,[6] centrifugation-based methods,[7] gas-based methods,[8] electrospinning,[2a,9] 3D bioprinting,[10] template methods,[11] and sputtering methods[12] (**Figure 1**). Based on these strategies, the produced complex AMs are used in cell coculture,[13] micromotors,[14] microreactors,[15] multidrug release,[16] multienzyme tandem reactions,[17] multitarget detection,[18] microbarcodes,[19] biocolloidal,[20] sensors,[21] medical imaging,[22] tissue repair,[23] and so on.

The aforementioned applications highlight the need to integrate multifunctional materials into AMs. In this review, we present and compare the methods used to fabricate AMs. We then examine recent applications of AM systems, including cell coculture, drug delivery, microrobots, and scaffold building. The primary objective of this review is to highlight the biomedical potential of these microcarriers and offer guidance on their fabrication and characterization methods. With the increasing literature on AMs, we believe that AMs will gain interest across a broader

range of application areas. This review summarizes the most recent scientific information on AMs and their applications in various fields, with a particular emphasis on biomedical applications.

2. Fabrication Strategies of AMs

The precise fabrication of morphological microstructures is critical because the micrometer-scale structural details of anisotropic morphologies can significantly affect their properties and performance. AMs can be generated using top-down methods, such as surface modification and incorporation of different chemical functional groups, and bottom-up technologies, including seeded emulsion polymerization, template formation, and self-assembly approaches.[24] The bottom-up approach is economical and highly efficient compared to the top-down approach.[24a,25] AMs with numerous morphologies and dimensions can be generated via several strategies, including microfluidics, lithography, 3D printing, electrospinning, centrifugation, gas, and template.[26] A comprehensive understanding of the fabrication of AMs is essential to effectively utilize their characteristics and explore their applications. In this section, we summarize the methods used to fabricate AMs with typical anisotropic morphologies and properties.

2.1. Microfluidics Strategy

Microfluidics technology is a powerful approach and extensively explored for the fabrication of AMs, including particles and fibers, enabling unprecedented control of their morphology and complexity over the past few decades.[27] In microfluidics, the properties of immiscible fluids are consistently utilized at the microscale to form and control droplets that can subsequently be crosslinked into AMs. The primary mechanism of microdroplet formation in these microfluidic devices involves an immiscible continuous oil phase that shears the dispersed phase flowing through the microchannel during fabrication. An initiator or crosslinker is used to crosslink the prepolymers, whereas a surfactant is used to stabilize the emulsion.[21a] Typically, to create complex AMs that fulfill the intricate demands of biomedical applications, microfluidic chips made of polydimethylsiloxane (PDMS) and capillaries are required, enabling the precise control of fluidic elements at the microscale. Microfluidic junctions are created using microfabricated molds made of PDMS, which can be customized to adjust their morphology and size. Capillary-based microfluidic equipment, consisting of glass capillaries arranged in a coaxial manner, either in a coflow or flow-focusing configuration, can generate microfluidic emulsions that are then cross-linked into AMs. The primary advantage of microfluidic technologies lies in precise control over the droplet formation process, which can be achieved through the design of microfluidic channels with predetermined geometries and regulation of input parameters such as flow rates. Notably, by varying the intersection geometry and relative flow rates of multiple phases, the droplet diameter can be effectively regulated within the micrometer range of a few micrometers to hundreds of micrometers. Monodisperse populations of particles with dispersity indices as low as 1–2% were also generated.[28] Additionally, microfluidic methods have been extensively used to fabricate AMs across a diverse range of polymers, including polyethylene glycol (PEG), gelatin methacryloyl (GelMA), sodium alginate (SA), chitosan, gelatin, and agarose.[29]

Microfluidic methods impose two critical conditions on prepolymer precursor solutions. The solution must possess relatively low viscosity to enable smooth pumping through narrow microchannels. Furthermore, the droplets should crosslink rapidly during collection to avoid aggregation. Numerous technologies have been developed to crosslink droplets, including polymerization, photocrosslinking, temperature-induced gelation and freezing, ionic crosslinking, and phase separation.

In this discussion, we focused on the fabrication of complex microparticles and their morphologies, including anisotropic particles (APs) and anisotropic fibers (AFs) (Table S2, Supporting Information). For instance, Janus APs were typically generated by introducing two aqueous solutions into a main junction under laminar flow, followed by the formation of droplets through additional flow focused at the secondary emulsion junction (**Figure 2A,B**).[30] Additional aqueous solutions can be used to create multicompartmental microspheres. Zhao et al. fabricated a four-faced photonic crystal microsphere using four aqueous solutions (Figure 2C).[5a] The preparation of more complex and irregular APs was also explored. Yin et al. proposed a magnetic-directed assembly technology for creating a variety of molecular-analog photonic crystal cluster particles, including tetrahedral and triangular bipyramid configurations, based on microfluidics (Figures 2D).[5b]

Compartments can be prepared through phase separation within droplets even in the absence of multiphasic droplet templates. The evaporation-induced phase separation in drops is a versatile method for creating multiple domains within a single carrier. For instance, the solution containing two distinct polymers was emulsified in water, resulting in monodisperse microgels (micrometer-scale granular hydrogels) with dual compartments after crosslinking. Phase separation can be permanently captured by photopolymerization of polymer precursors, resulting in APs. Phase separation can create core–shell and Janus structures, enabling the one-step encapsulation of multiple components at the desired position. The aqueous poly(ethylene glycol) diacrylate (PEGDA) solution turned purple upon loading blue and red dyes. Following the addition of separating agent to the mixture to induce phase separation, blue and red dyes were transferred to the core and shell regions (Figure 2E).[31] Moreover, phase separation can be used to generate APs with complex structures. As shown in Figure 2F, Min et al. proposed a strategy that was closely related to the properties of the two-phase polymers, solvents, and microenvironment.[32] APs with diverse morphologies can be obtained using various polymers and external microenvironments.

Another interesting microfluidic strategy for fabricating APs typically uses droplet-in-droplet templates to design the internal compartments. Precise control of microfluidics regarding the quantity, size, and ratio of different inside droplets allows for accurate regulation of the internal structure of the microparticles and encapsulation characteristics of different components. The inner and innermost droplets can function as separate compartments for the encapsulation of both oil- and water-soluble substances. Using quadruple emulsions as templates, a variety of multicompartment structures can be engineered

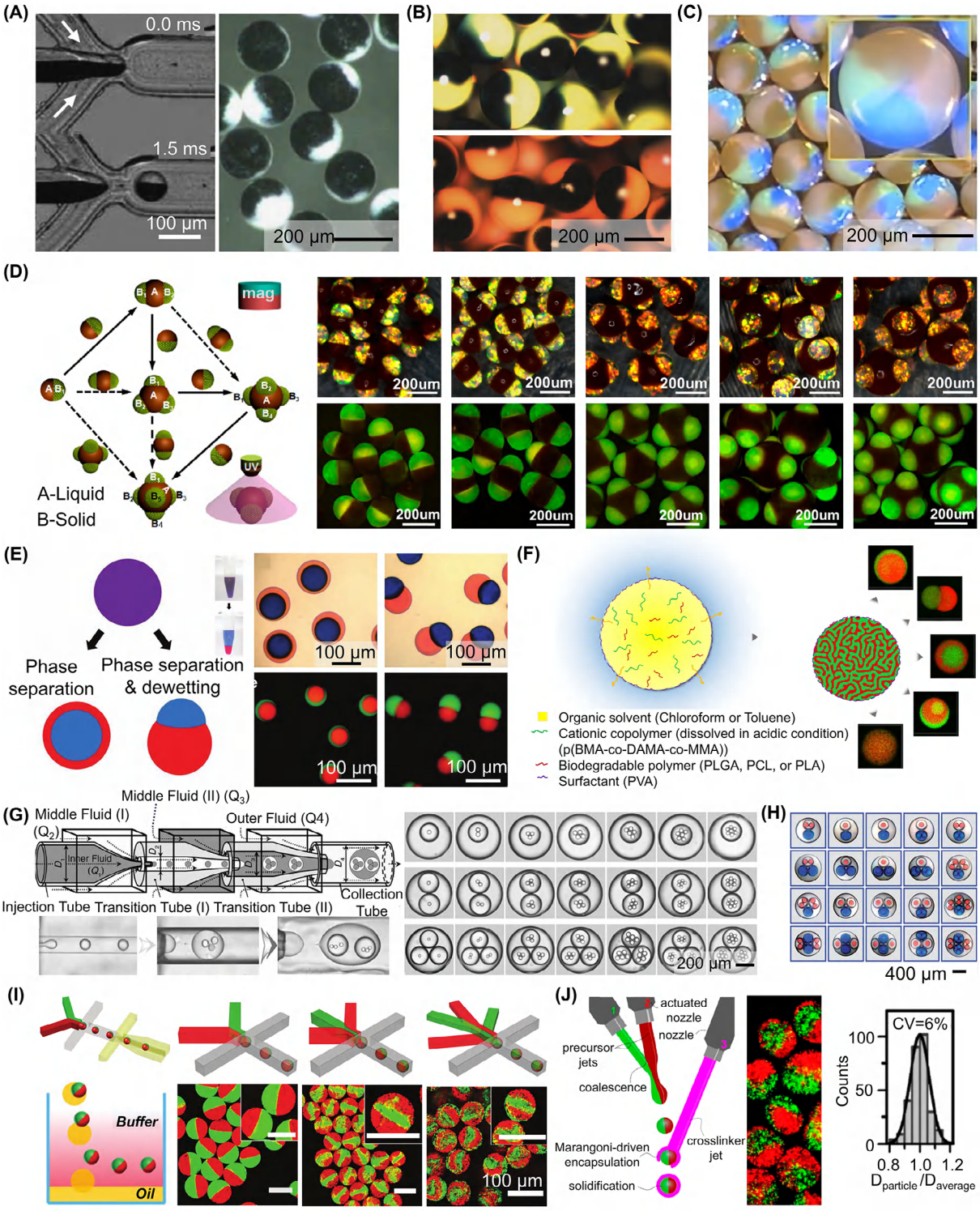

Figure 2. Microfluidic production of APs. A,B) Fabrication of Janus AMs at the sheath-flow junction. Adapted with permission.[30a] Copyright 2004, Elsevier. Adapted with permission.[30b] Copyright 2008, Wiley-VCH. C) Fabrication of four-faced photonic crystal microspheres using four aqueous solutions. Adapted with permission.[5a] Copyright 2013, American Chemical Society. D) Anisotropic photonic crystal clusters constructed from solid–liquid Janus building blocks. Adapted with permission.[5b] Copyright 2016, American Chemical Society. E,F) Microfluidic production of uniform AMs through phase separation in emulsion drops. Adapted with permission.[31] Copyright 2013, Wiley-VCH. Adapted with permission.[32] Copyright 2016, American Chemical Society. G,H) Capillary microfluidic device and formation of precisely controlled monodisperse double emulsions. Adapted with permission.[33a] Copyright 2007, Wiley-VCH. Adapted with permission.[33b] Copyright 2011, Royal Society of Chemistry. I) Fabrication of APs with independently controlled compartments using microfluidics. Adapted with permission.[13a] Copyright 2018, Wiley-VCH. J) Generation of APs using channel-free microfluidics. Adapted with permission.[35] Copyright 2018, American Chemical Society.

(Figure 2G,H).[33] These microfluidic strategies provide new opportunities for designing core–shell-based APs, allowing for controlled and separate coencapsulation of various substances and the release of these components on demand through various activation mechanisms.

Although these representative studies prepare complex microparticles through sophisticated processes, their applications in specific fields encounter challenges.[33b,34] Moreover, their application in the field of biology is still limited because the use of ultraviolet (UV)-irradiation, crosslinkers, photoinitiators, oils, and surfactants is unnecessary. To overcome this limitation, Zhang et al.[13a] proposed a microfluidic strategy for producing monodisperse APs with independently controlled compartments that could encapsulate cells and facilitate their controlled assembly within a micrometer-sized space (Figure 2I). They produced APs through a two-step method, namely, the preparation of microparticles using an oil–water strategy. The microgels were immediately transferred from the oil in which they were fabricated to an aqueous continuous phase through the rapid crosslink of the precursor solutions and dissociation of the surfactant. A promising alternative is research on air microfluidic equipment to form compartmental AMs without relying on oil. For instance, a gas-shearing or centrifugal force is typical in air microfluidics (Figure 2J).[35]

Previous studies have reported the fabrication of AFs using microfluidics. These microfibers were continuously generated by employing multiple laminar flows in multibarrier capillary microfluidics. AFs are long, thin, and flexible materials characterized by anisotropic structures, various compartments, and heterogeneous components. They further address various applications in disease modeling, cannular tissue engineering, creation of various functional 3D objects, and pharmaceutical screening.[36] The morphology of AFs can be designed from simple to complex by merely altering the arrangement of the capillaries and switching the running channels. Cheng et al.[13b,37] proposed a multiple laminar-flow microfluidic strategy for the preparation of AFs with adjustable properties, morphologies, and structures (**Figure 3A,B**). A range of heterogeneous or anisotropic cell-laden hydrogel microfibers were generated by adjustable structural and morphological characteristics derived from multiple specifically designed injection flows. Furthermore, the same research group introduced a coaxial capillary microfluidic method with consecutive spiraling and spinning features for scalable production of helical microfibers.[38] Helical microfibers featuring novel core–shell, triplex, and Janus structures were fabricated by altering the design of the capillaries in the chips (Figure 3C). In a particularly compelling application of this strategy, Yu et al.[38] developed a cardiac sensor that utilized helical microfibers as force indicators for monitoring cardiomyocyte contractions. In addition to capillary-based approaches, chip-based methods are frequently used to generate AFs. For instance, a simple chip-based microfluidic strategy has been presented for the manipulation and continuous spinning of hollow microfibers. These microfibers were characterized by their intricate structural and morphological features, as well as their heterogeneous composition (Figure 3D).[39] They also proposed the construction of 3D microtissues with complex biochemical cues via the selective incorporation of active molecules, large protein factors, and cells into AFs, functioning as active composites, thereby opening new avenues for tissue engineering applications. A spinning technology was proposed that integrated a digital fluid control system with a microfluidic chip.[19a] By incorporating active functional modulations, such as altering the flow through a digital control scheme, they produced AFs with diverse chemical compositions that could be spatiotemporally coded (Figure 3E). The coding resolution across the fiber was a few micrometers and could be regulated to a few hundred micrometers along the fiber. Another strategy for fabricating coded AFs was proposed by Yu et al., who introduced a wet-spinning process integrated with a droplet microfluidic approach for the one-step formation of multifunctional AFs.[40] A range of spherical materials with diverse characteristics, such as polymer microspheres, cell microspheres, and hydrophobic microdroplets, can be introduced into AFs for further applications (Figure 3F). Overall, the uniqueness of this series of approaches lies in their simplicity, flexibility, and controllability. These forms of AFs, which differ in composition, configuration, and biocompatibility, show significant potential for applications in regenerative medicine and materials science.[41]

2.2. Lithography

AMs can also be fabricated using lithographic methods, and most studies have focused on microparticle fabrication. Lithography technologies include photobleaching, flow lithography, soft lithography (e.g., microcontact printing), and holographic lithography. Photobleaching and flow lithography are commonly employed to fabricate anisotropic microparticles (Table S3, Supporting Information).

Spatially selective photobleaching can produce APs with different patterns by inscribing designs onto fluorescently dyed microparticles. In contrast to other single-step methods, this secondary processing method is used to prepare the APs. The designed patterns can be inscribed within a microsphere that is uniformly dyed with fluorescence through spatially selective photobleaching. Photobleaching is a light-induced process wherein fluorescent molecules lose their fluorescence characteristics, resulting in diminished fluorescence intensity. Any geometry, including symbols or barcodes, can be bleached (**Figure 4A**).[42] This method has been effectively utilized with polyethylene glycol-grafted polystyrene, polystyrene, and dextran microparticles. The flexibility of this method makes it ideal for high-throughput screening and counterfeiting applications. To enhance the practical applicability of these microparticles in anticounterfeiting drugs, labeling the drug itself rather than its packaging would represent a significant advancement in combating counterfeiters. The code is inscribed in the central plane of a digitally encoded microparticle (memobead), which is depth-dependent.[43] As shown in Figure 4B, the code is clearly visible in the bleached layer; however, at different depths within the memobead, it becomes unreadable. Microparticles have been incorporated into drug tablets.

The continued advancement in microfluidics has led to the emergence of flow lithography.[44] Specifically, flow lithography can be categorized into two distinct types: stop-flow lithography (SFL) and continuous-flow lithography (CFL). The main difference between them is the relative motion of the mask and hydrogel. Typically, a polymer precursor is introduced into a templated

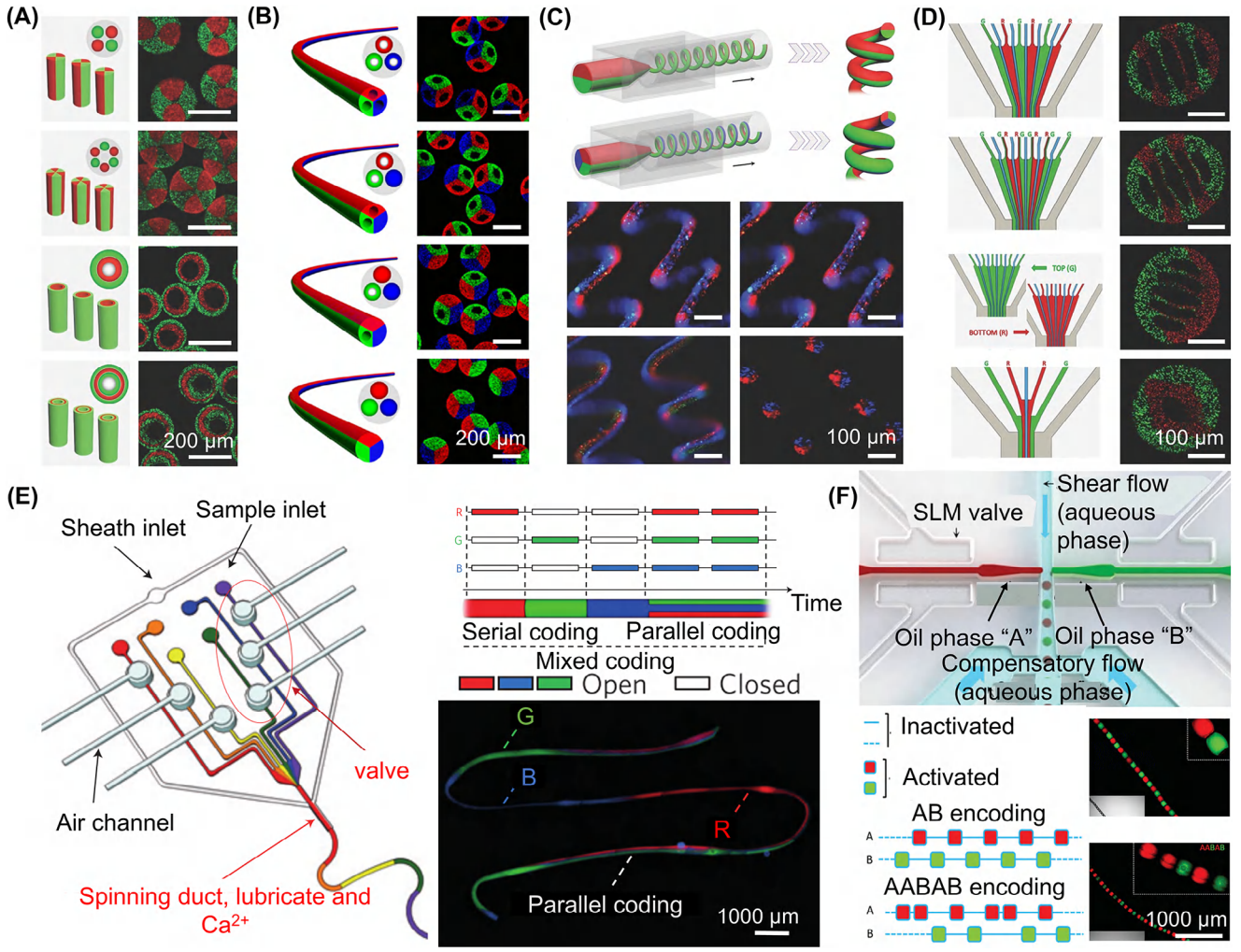

Figure 3. Microfluidic production of AFs. A, B) Generation of multicompartmental fibers with microfluidics. Adapted with permission.[13b] Copyright 2014, Wiley-VCH. Adapted with permission.[37] Copyright 2016, American Chemical Society. C) Fabrication of helical microfibers from microfluidics. Adapted with permission.[38] Copyright 2017, Wiley-VCH. D) Fabrication of heterogeneous hollow microfibers using a PDMS chip. Adapted with permission.[39] Copyright 2016, Wiley-VCH. E) Preparation of AFs with diverse chemical compositions via a microfluidic chip combined with a digital fluid controller. Adapted with permission.[19a] Copyright 2011, Springer Nature. F) Fabrication of a biomimetic hybrid fiber with multiple functionalities by a droplet microfluidic approach combined with a wet-spinning process. Adapted with permission.[40] Copyright 2014, Wiley-VCH.

mold channel containing the negative features of the desired APs for crosslinking, followed by curing. Normally, hydrogels are solidified at the microscale through photopolymerization. In SFL, the hydrogel and mask stop moving before exposure and continue to move to the next position after hydrogel crosslinking.[45] In CFL, the hydrogel and mask keep moving, and photopolymerization occurs during motion.[46] As a result, SFL offers greater resolution, whereas CFL provides increased throughput. Doyle et al.[6a] prepared APs for high-throughput biomolecular analyses (Figure 4C). Encoding and probing were integrated into a single process to produce multipurpose APs containing over one million distinct codes. In addition to using unique materials as codes, codes could also be derived using multiple color-based materials and structural colors, resulting in exceptional coding capabilities. For instance, Kwon and co-workers[47] used a color-tunable magnetic material to produce colored APs with multiaxis rotational control, as shown in Figure 4D. Color-barcoded APs offer a coding capacity that extends to billions with unique magnetic handling capabilities enabled by color-tunable magnetic materials. The main advantage of lithography technologies is the precise control over the geometrical features of the mask or mold channel, leading to excellent control over the geometry and monodispersity of APs. Similarly, as shown in Figure 4E, Lee et al.[48] reported an encoding technology that integrated near-infrared excitation, decoding, and spatial patterning to distinguish particles synthesized using flow lithography.

Despite advancements in microfabrication technologies that have enabled the fabrication of mold channels and masks featuring micrometer-scale details, generating APs with specific external and internal structures has been challenging. Flow lithography methods encounter the practical challenge of extracting crosslinked APs from a mold channel, which restricts the complexity of the external or internal properties that can be achieved.

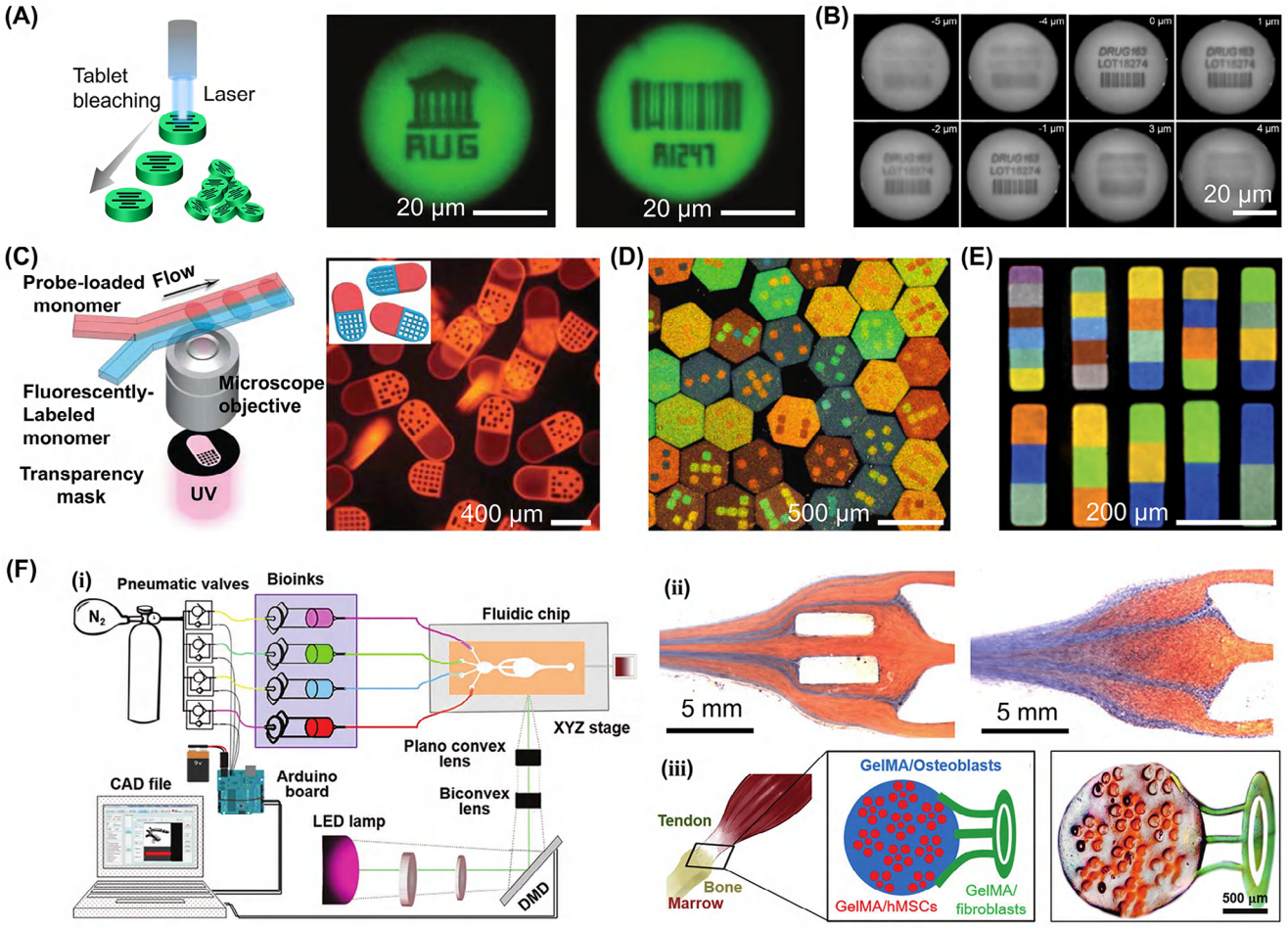

Figure 4. Fabrication of AMs with lithography. A) Fabrication of APs with different patterns by spatial selective photobleaching. Adapted with permission.[42] Copyright 2003, Springer Nature. B) Preparation of digitally encoded drug tablets. Adapted with permission.[43] Copyright 2007, Wiley-VCH. C) APs for high-throughput biomolecule analysis. Adapted with permission.[6a] Copyright 2007, American Association for the Advancement of Science. D) Preparation of colored APs with multiaxis rotational control using a color-tunable magnetic material. Adapted with permission.[47] Copyright 2010, Springer Nature. E) Luminescence images of poly(urethane acrylate) particles containing upconversion nanocrystals. Adapted with permission.[48] Copyright 2014, Springer Nature. F) Fabrication of multimaterial APs via maskless stereolithographic bioprinting. Adapted with permission.[50] Copyright 2018, Wiley-VCH.

Two-photon light sources facilitate the production of APs with complex 3D geometries. For instance, polymeric microtubes with intricate geometries and high aspect ratios can be synthesized using two-photon vertical-flow lithography.[49] A major drawback of lithography approaches is their low throughput compared to alternative methodologies. The throughput efficiency is constrained by the dimensions of the mold channel or masks, the objective, and the light source. Flow-lithography technologies provide the most significant throughput because they can be parallelized with microfluidic technologies.

In addition to photomasks, other types of maskless lithography have been used to produce APs. Zhang and co-workers[50] employed a maskless stereolithography-based platform to fabricate hydrogel APs. The microfluidic device can rapidly alternate between different hydrogel solutions to produce layer-by-layer APs with high spatial resolution (Figure 4F). APs generated using lithographic methods that do not utilize oil or surfactants are suitable for cell encapsulation. To approve the biocompatibility of this system, cell-laden GelMA was introduced into the microfluidic device, fabricating cellularized APs. Three distinct cell categories (mesenchymal stem cells (MSCs), fibroblasts, and osteoblasts) were loaded into the APs to replicate the structure of the musculoskeletal interface. Furthermore, structural color, which showcases the inherent beauty of many plants and animals, offers advantages such as ease of fading, nontoxicity, and environmental friendliness. This characteristic has broad application prospects in anticounterfeiting, functional material construction, and biological/chemical detection.[51] Kim et al.[52] employed maskless lithography with color-tunable magnetic materials to fabricate photonic crystal-based APs with different bandgaps. Photonic crystals with varying bandgaps were fabricated within a few seconds on different substrates.

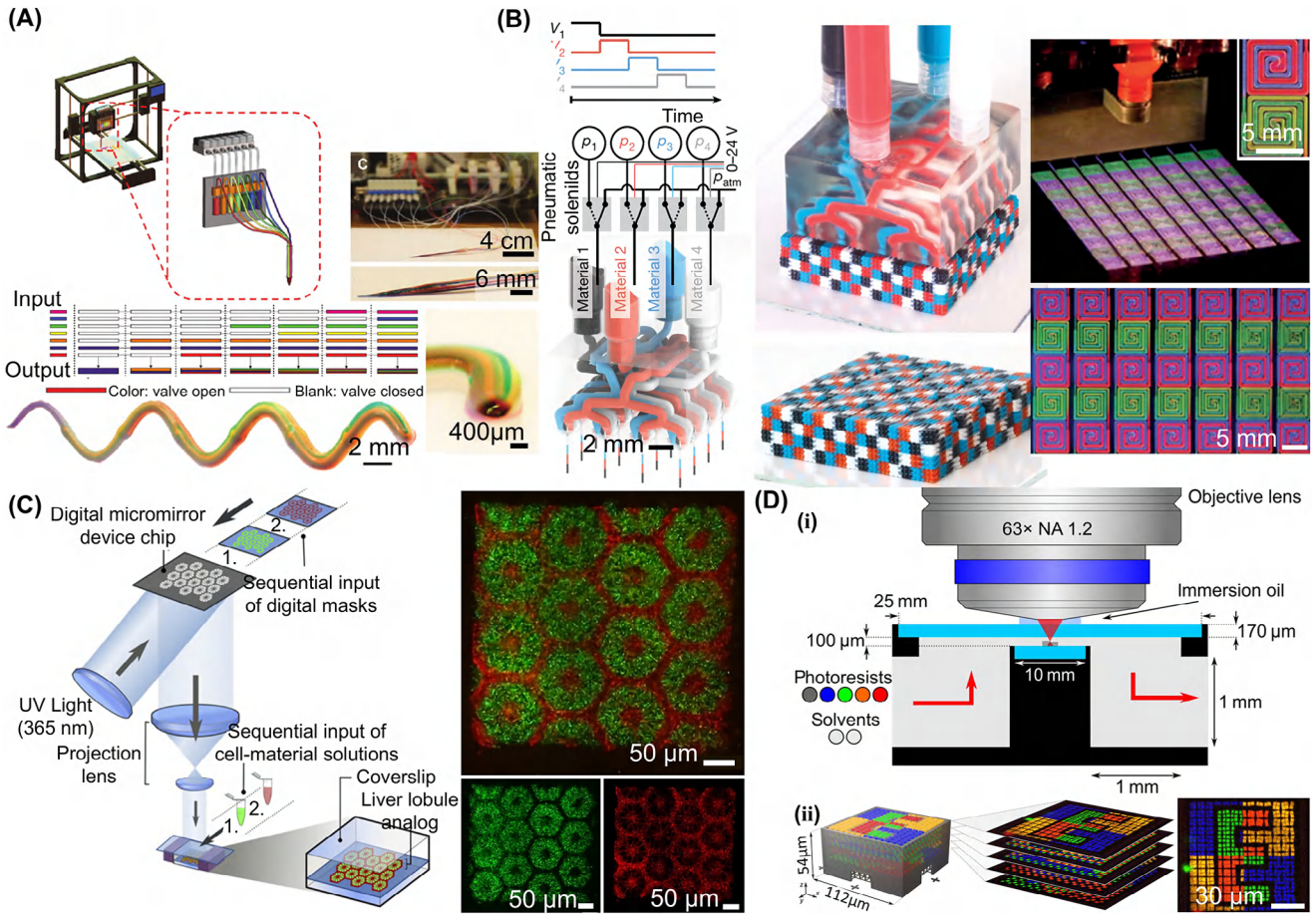

Figure 5. 3D bioprinting methods for preparation of AMs. A) The bioprinting device formed multicompartmental microfiber consisting of one to seven bioinks in different spaces. Adapted with permission.[56] Copyright 2017, Wiley-VCH. B) Fabricating complex voxelated soft matter via multimaterial multinozzle 3D printing in a layer-by-layer manner. Adapted with permission.[57] Copyright 2019, Springer Nature. C) Printing of iPSC-derived hepatic model with customized DLP-based 3D bioprinting system. Adapted with permission.[60] Copyright 2016, National Academy of Sciences. D) (i) Schematics of fabrication of AMs using laser lithography apparatus integrated with a multiple-channel chamber. (ii) Seven different liquids for fabrication of complex 3D AMs. Adapted with permission.[61] Copyright 2019, American Association for the Advancement of Science.

2.3. 3D Printing

3D printing and bioprinting are among the most advanced technologies, key components of numerous research fields, particularly biomedical engineering,[53] and used to fabricate AMs with designed shapes.[54] Several 3D bioprinting modalities have been developed, including valve-based printing, extrusion-based printing, acoustic encapsulation, light-based printing, and inkjet-based printing, which enabled the fabrication of different shapes with simple to complex geometries.[55] In contrast, multimaterial extrusion bioprinting and light-based 3D printing can be used to fabricate a much broader range of AMs. Zhang and co-workers[56] reported a multimaterial extrusion bioprinting platform that could smoothly switch and continuously extrude multiple coded bioinks to rapidly fabricate AMs. As shown in **Figure 5**A, the bioprinting device fabricated a continuous multicompartmental microfiber consisting of one to seven bioinks in different spaces. In addition to achieving the biofabrication of AMs at a high speed, the authors also demonstrated the ability of their bioprinter to form gradient and complex constructs for applications in tissue engineering. Lewis and co-workers[57] designed printheads and implemented high-frequency switching of perfusion channels to extrude ultracomplex AMs through multimaterial multinozzle 3D printing layer-by-layer. As shown in Figure 5B, this strategy can be used to fabricate complex voxelated soft matter with the composition optimized for the functionality and structure of materials designed at the voxel scale. Furthermore, in 3D printing, the integration of stereolithography and multimaterial fluids allows the precise fabrication of complex multicomponent structures, creating a robust platform for printing multimaterial microstructures.

Light-based printing is an essential method for AM generation.[58] Light-based 3D printing has consistently generated highly elaborate cellularized constructs with tissue-scale features that could not be obtained using layer-by-layer methods.[59] Numerous tissues and organs have complicated structures. For instance, a significant challenge in creating an in vitro liver model stems from the limitations of existing methods in accurately replicating the intricate liver microenvironment shaped by its complex microarchitecture and diverse

cell combinations. From this perspective, to replicate tissues and organs by combining 3D bioprinting method with regenerative medicine and tissue engineering, Ma et al.[60] developed microscale hepatic AMs composed of supporting cells and liver cells (Figure 5C). This model facilitated both the functional and structural enhancement of hepatic progenitor cells, making it suitable for drug screening and liver pathophysiology studies in vitro. Wegener and co-workers[61] utilized a system that incorporated a multiple-channel chamber within a laser lithography apparatus to fabricate AMs, as shown in Figure 5D(i). In contrast to traditional methods, this device eliminated the need for repeated trips between the lithography equipment and precuring solution, and could directly create target AMs based on a programmed design, which significantly facilitated the manufacturing of complex structures consisting of AMs. The authors further printed complex 3D AMs, which comprised five diverse photoresists, using seven diverse liquids for formation within the laser lithography system (Figure 5D(ii)).

2.4. Electrohydrodynamic (EHD) Cojetting

The EHD cojetting method is frequently used to fabricate AMs and AFs by applying high voltages to polymer solutions.[62] During the EHD cojetting process, voltage was applied to the needle tip of the syringe. While the pump maintained a continuous flow of the solution, charges gathered at the surface of the hydrogel precursor solution. Once the applied voltage surpassed a critical threshold, it overcame the surface tension at the tip of the needle, resulting in a charged liquid column or a jet of droplets collected on the substrate. By controlling the parameters of the polymer solutions (viscosity, conductivity, and concentration) and flow device, multifarious compartmentalized AFs or AMs could be prepared, exhibiting various shapes and compositions, including core/shell shapes to Janus-type (Table S4, Supporting Information).[9b,63] The EHD cojetting method, mainly developed by Lahann and co-workers, is a modified electrospray process.[2a] As one of the most commonly used technologies for forming AMs, the strategy allows cost-effective production of anisotropic fibers and particles across a broad range of sizes, specifically from 0.1 to 100 µm. As shown in **Figure 6A**, Bhaskar and Lahann[64] used this approach to prepare Janus-, tri-, or even multicompartmentalized fibers with side-by-side needle configurations. They also fabricated compartmentalized microhelical fibers by designing a collection that rotated in two dimensions (Figure 6B).[9b] Huang et al. fabricated encoded fibers through the spatially selective photobleaching of electrospun fibers, i.e., a secondary processing method (spinning and bleaching) used to prepare APs (Figure 6C).[65] Moreover, compartmentalized fibers can be used to fabricate cylindrical APs by cutting them after rotating the collection, as shown in Figure 6D.[66] APs can achieve chemically controlled bending via asymmetric expansion, which generates surface stresses because different compartments are loaded with dissimilar materials.[67] In addition, APs can be surface modified by the covalent attachment of cell-adhesion peptides to achieve phase-selective cell attachment on a single microcylinder.[68] The prepared particles undergo secondary deformation through external induction. For instance, it can be induced to form circles and curves (Figure 6E).[69] In addition to using fiber cutting to prepare microparticles, the EHD cojetting system can directly fabricate APs.[70] Typically, APs are composed of biphasic or triphasic Janus particles, as shown in Figure 6F,G.[2a,71]

2.5. Centrifugation

In 2007, centrifuge-based technologies were introduced. Haeberle et al.[72] used the centrifugal technology to produce highly monodisperse droplets. Oils and surfactants were also used during the fabrication process. In 2012, Maeda et al. documented the preparation of multicompartmental APs of uniform size by integrating a centrifugation-based system with a multibarreled capillary (**Figure 7A**).[7b] This method differs from previous centrifugal technologies and mainstream microfluidic systems; it relies solely on droplet formation achieved through ultrahigh gravity, without the need for oils, surfactants, or UV light. The experimental configuration involved three key components: fluorescently labeled polymer solutions loaded into multibarrel capillaries, a capillary array secured by an acrylic fixture within microtubes containing $CaCl_2$ solution, and a collection bath that included a crosslinker. During centrifugation, centrifugal acceleration propels the solutions through the capillary orifices, inducing hydrodynamic flow segmentation at the capillary tips. Following droplet generation, immediate ionic crosslinking occurs in the collection bath. The partitioning and dimensions of the APs can be easily modified through adjusting the capillary architecture. However, centrifugation-based systems are limited in their ability to fabricate spherical APs. Nonequilibrium-induced microflows (diffusion and Marangoni flows) were introduced to fabricate APs with high morphological complexity from the centrifugation-based system, as illustrated in Figure 7B.[73] They further enhanced the morphological complexity by the selective disintegration of specific compartments of APs.

2.6. Gas-Based Method

Recently, gas-based methods have been proposed for the fabrication of APs to broaden their applications in biomedical engineering. This method exclusively utilizes the gas flow to assist generation of droplets ("gas-shearing") and is designed for the extensive production of monodispersed APs without using oil, surfactants, or UV.[74]

The preparation of microparticles by gas-shearing was first reported by Anilkumar et al.[75] in 2001. For decades, gas-based methods have been used to prepare particles with diverse structures and applied in various fields.[76] However, preparing multicompartmental anisotropic microparticles is challenging owing to the unstable nature of the gas. Tang et al. successfully designed microspherical APs via gas-shearing using an in-house coaxial needle device and removed oils, i.e., several needles were positioned coaxially within a shell.[77] Shear forces induced by nitrogen gas flowing through the gap between the inner needle and shell effectively assisted in the generation of polymeric droplets. When the shear force of nitrogen was greater than the surface tension, a microdroplet was formed. The collecting bath, including the crosslinker, solidified the polymeric droplets into solid microparticles. By adjusting the setup of the needle device and

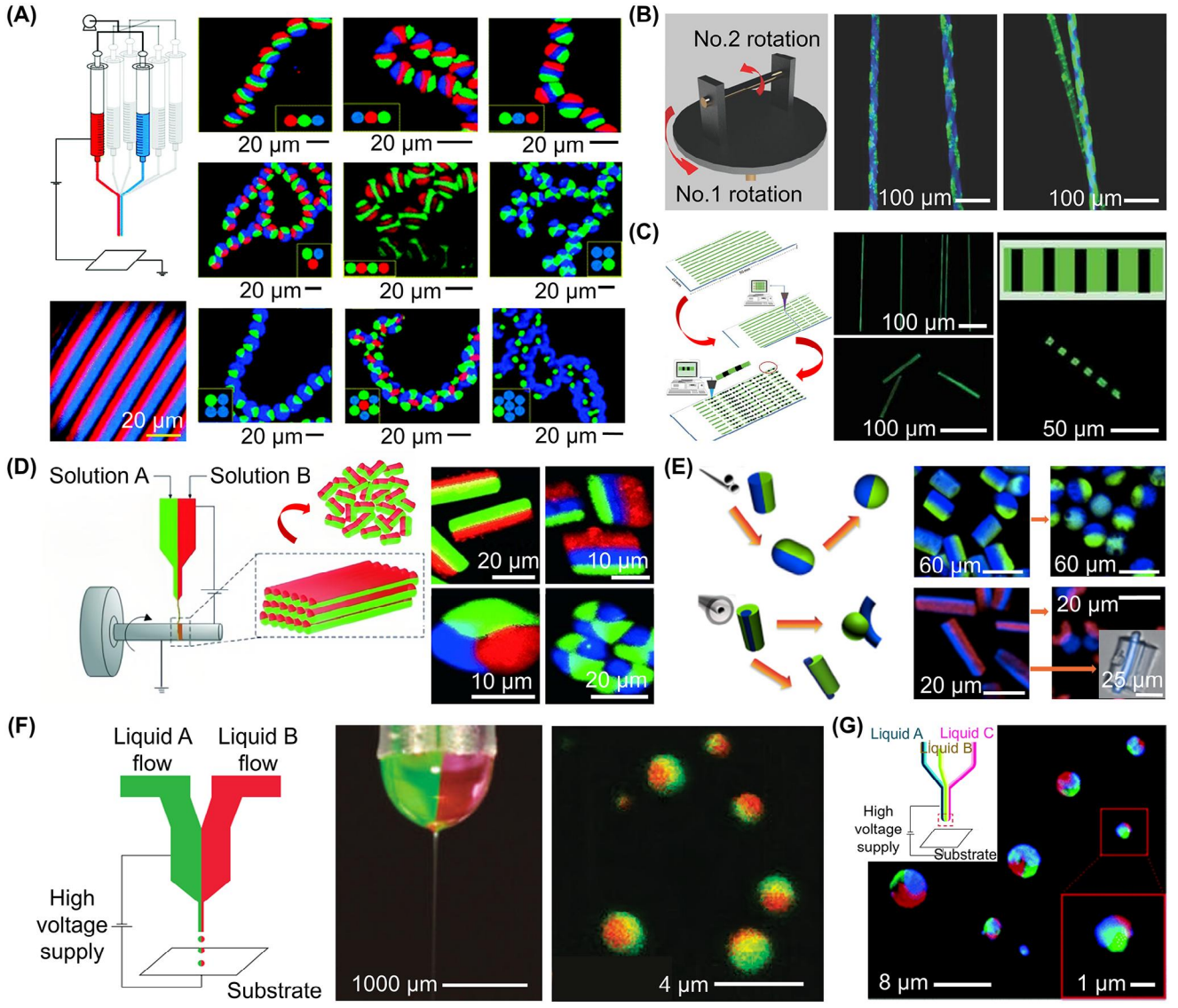

Figure 6. Electrohydrodynamic (EHD) cojetting for preparation of AMs. A) Janus-, tri- or even multicompartmentalized fibers with side-by-side needle configurations prepared by EHD cojetting system. Adapted with permission.[64] Copyright 2009, American Chemical Society. B) Bicompartmental microfibers twisted in situ to form helical microfibers during EHD cojetting. Adapted with permission.[9b] Copyright 2018, John Wiley and Sons. C) Preparation of encoded fibers by secondary processing method. Adapted with permission.[65] Copyright 2010, Wiley-VCH. D) Rod-shaped particles with controlled sizes, aspect ratios, shapes, and surface chemistry. Adapted with permission.[66] Copyright 2009, Wiley-VCH. E) The particles undergo secondary deformation through external force induction and are induced into circles, curves, etc. Adapted with permission.[69] Copyright 2012, National Academy of Sciences. F,G) The EHD cojetting system fabricated biphasic (F) or triphasic (G) particles directly. Adapted with permission.[2a] Copyright 2005, Springer Nature. Adapted with permission.[71] Copyright 2006, American Chemical Society.

the nitrogen flow, the gas-based method enabled the straightforward control of particles with 2–8 compartments, allowing for a flexible design regarding the characteristics of each compartment (**Figure** 8A). The gas-based method is highly cytocompatible because oils or surfactants are not used. Based on a previous strategy, Tang et al.[78] successfully prepared ten-faced microspherical barcodes (Figure 8B). The color of each compartment was programmed using ten multicompartment microparticles. More importantly, the technology was expected to enhance the food and pharmaceutical anticounterfeiting domains owing to its high biocompatibility. In addition to gas-shearing strategies, another gas-based method for fabricating APs has been developed. Zhao et al.[8a] used a microfluidic nozzle to print versatile spiral microarchitectures inside microspheres with airflow assistance, directly permitting the one-step fabrication of spherical helical structures (Figure 8C).

2.7. Templating Method

Template-based approaches are effective for AP production. Most templating methods use a micropatterned master mold to

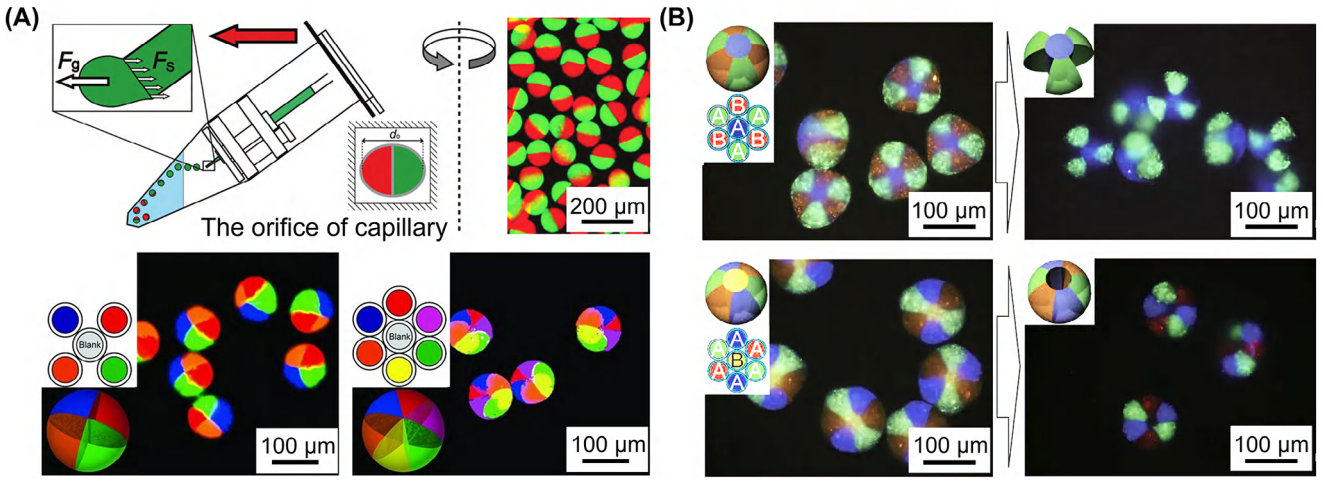

Figure 7. Centrifugation methods for fabrication of AMs. A) APs formation depends only on air-liquid droplet formation provided by ultrahigh gravity. Adapted with permission.[7b] Copyright 2012, Wiley-VCH. B) High complex morphology of APs fabricated via nonequilibrium-induced microflows such as the diffusional and Marangoni flow. Adapted with permission.[73] Copyright 2016, Springer Nature.

generate replicates. The morphological characteristics of the mold directly influence the shape of the fabricated APs. During the fabrication process, polymer precursors are cast onto master molds composed of materials, including but not limited to glass, PDMS, or silicon substrates.[11b,79] Notably, Zhang et al.[27] pioneered the development of a nonwetting template-assisted particle replication technique. This approach enabled the production of monodisperse 2D APs with enhanced control over sizes (**Figure 9A**). However, the morphology of the APs prepared using template-based techniques is constrained by the predefined geometry of the mold. To address this constraint, Choi et al.[11b] recently proposed modified template-assisted strategies for the controlled fabrication of engineered APs (Figure 9B). They proposed a two-step template-based technology to generate uniform APs.[11a] Specifically, the fabrication process entailed the sequential generation of primary and secondary compartments within molds, utilizing surface tension-induced droplet production integrated with photopolymerization. Secondary compartment formation was accomplished by repeating Step 1. The subsequent assembly of the primary and secondary components, followed by UV-induced polymerization, yielded monodisperse multicompartmental APs. Furthermore, altering wettability facilitated the fabrication of core–shell APs with controlled compartmentalization. As shown in Figure 9C,[80] an alternative template-based technique that leveraged simple mold swelling and capillarity tuning was introduced to form intricate 3D APs from 2D molds. This process involved: 1) infiltration of a PEGDA photocurable solution into 2D molds, followed by 2) infusion of immiscible wetting fluids to induce structural deformation through mold swelling and tunable capillarity. Furthermore, they expanded their investigation to generate highly complex 3D microstructures with multiple compartments.

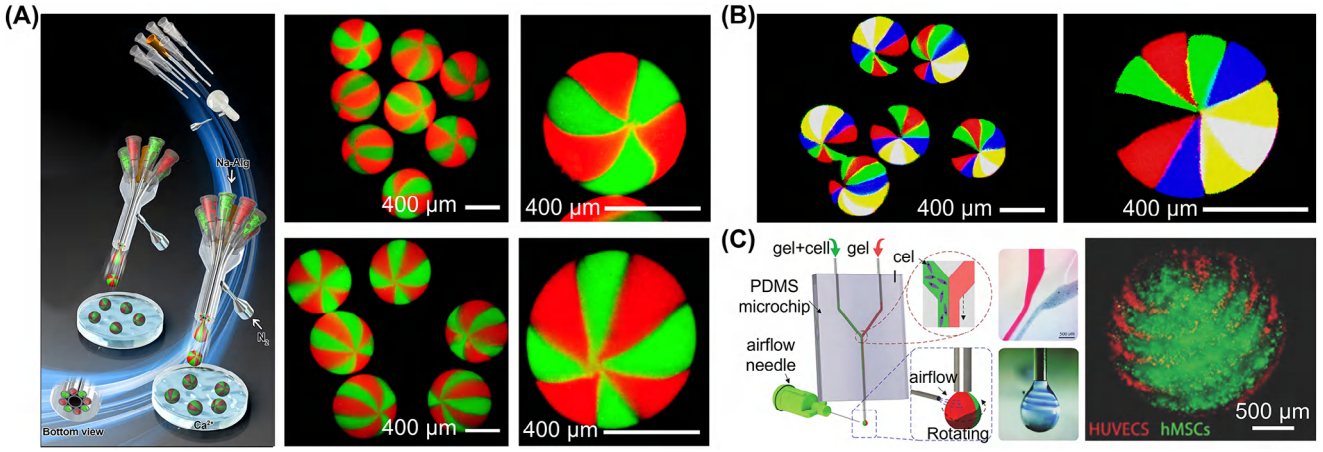

Figure 8. Preparation of AMs via gas-based methods. A) Multicompartment microparticles with precisely controlled properties can be used for magnetic microrobot and cell culture. Adapted with permission.[77] Copyright 2019, John Wiley and Sons. B) Ten-faced microparticle barcodes were used for food and pharmaceutical anticounterfeiting. Adapted with permission.[78] Copyright 2020, Wiley-VCH. C) Versatile spiral microarchitectures were printed inside the microparticles. Adapted with permission.[8a] Copyright 2018, Wiley-VCH.

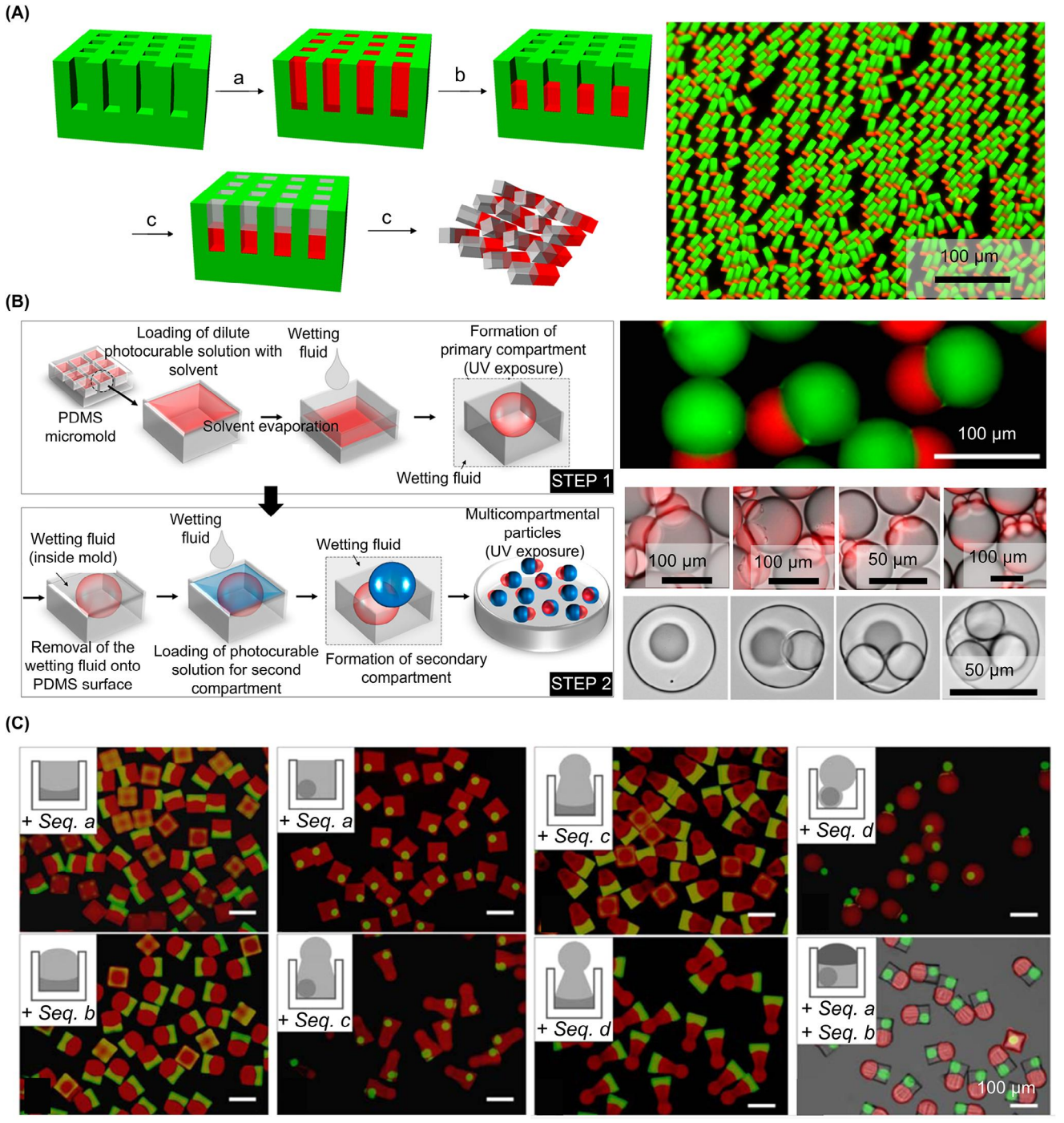

Figure 9. Fabrication of AMs by templating methods. A) Fabrication of APs in a nonwetting template. Adapted with permission.[27] Copyright 2009, IOP Publishing. B) Scalable fabrication of monodisperse multicompartmental via surface-tension induced droplet formation. Adapted with permission.[11a] Copyright 2015, American Chemical Society. C) Fabrication of 3D APs from 2D micromolds via simple tuning of wetting fluids. Adapted with permission.[80] Copyright 2015, American Chemical Society.

2.8. Sputter Coating Method

Sputtering coating is an important method for AMs with thin coating deposition. Highly uniform and dense multimaterial coatings can be prepared. Parameters such as air pressure and power precisely control the thickness. This method is usually applied to modify AM surfaces. For instance, spraying, sputtering, or deposition of metals on one side can be used to fabricate Janus microparticles.[81] Lee et al.[12b] proposed a novel category of photonic Janus microparticles that rendered magnetoresponse by iron deposition onto their surface and optical anisotropy though alternately sputtering two distinct dielectric

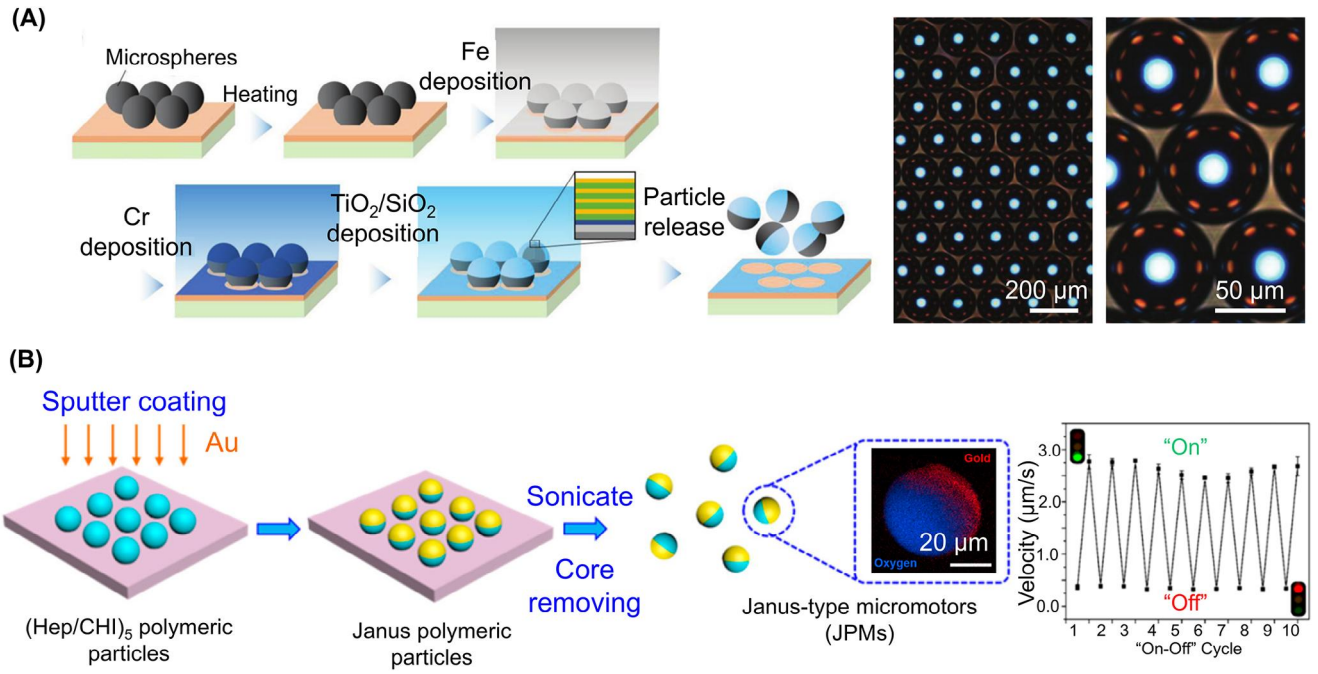

Figure 10. Fabrication of AMs through sputter coating methods. A) Photonic Janus microspheres with a gradient change of structural color. Adapted with permission.[12b] Copyright 2017, Wiley-VCH. B) Janus microrobots formed by sputter coating method. Adapted with permission.[82] Copyright 2018, American Chemical Society.

layers. The pronounced directionality and consistent flux of the sputter deposition led to a progressive variation in the thickness of the photonic layers on AMs, creating a gradient in the structural color. As the direction of the APs is determined by the orientation of the external magnetic field, the structural color can be moved or closed as required (**Figure 10A**). Similarly, the sputter coating method can be used to effectively fabricate microrobots. Heparin and chitosan were chosen as the base materials for the microparticles, with one surface coated with a gold shell (Figure 10B). Under near-infrared (NIR) irradiation, a local thermal gradient is formed. Based on the self-thermophoresis effect, the movement of these Janus microparticles can be easily controlled by varying the laser intensity and successfully applied to thrombus ablation.[82]

2.9. Other Methods

In addition to these strategies, other technologies have been employed to fabricate AMs. For instance, Luo et al.[83] proposed the use of superhydrophobic surfaces and the formation of controlled volumes of droplets, thereby creating AMs with multiple compartments characterized by diverse and precisely defined internal architectures. As shown in **Figure 11A** (top panel), the droplets solidified into templates via cooling induced agarose gelation. Subsequently, the calcium ions polymerized the SA molecules in the agarose network, resulting in hydrogel particles characterized by an agarose/SA double network. Consequently, multicompartmental structures within the hydrogel particles were formed by encapsulating the hydrogel particles within larger pregel droplets for subsequent polymerization (bottom panel in Figure 11A). To increase the manufacturing complexity of engineered hydrogel materials, as illustrated in Figure 11B, Chiang et al.[84] proposed a general technology for obtain 3D complex architectures. Specifically, programmable formation and assembly were performed on an electro-microfluidic platform using two electrical processes (electrowetting and dielectrophoresis). Using electric field control, researchers can selectively modify liquid-phase components to tailor the properties of microgels. These building blocks then undergo controlled assembly and crosslinking to form seamless heterogeneous hydrogel AMs. Cho et al.[85] proposed a sequential electrohydrodynamic processing methodology for engineering nonspherical hydrogel microparticles with discrete compartments. Consequently, the properties of each compartment can be easily adjusted. This was accomplished by varying the types or quantity of polymer and integrating distinct molecules into matrix (Figure 11C). Importantly, the resulting architectures demonstrated the simultaneous release of multiple growth factors at distinct release rates, enabled by the design of compartment-specific binding affinities.

In summary, the integration of innovative technologies and advanced materials has driven the development of AM strategies. Previous research on microfluidic strategies has shown great application potential owing to their exceptional capability to precisely control the AM morphology and structural complexity with high throughput, making them suitable for industrial scale-up.[86] However, the main problem with most microfluidic strategies is the low cellular activity owing to the residue of an organic solution. In addition, microfluidic chips are expensive owing to their precise structures. Lithography offers significant advantages for fabricating high-resolution complex 3D patterns; however, its scalability and applicability in

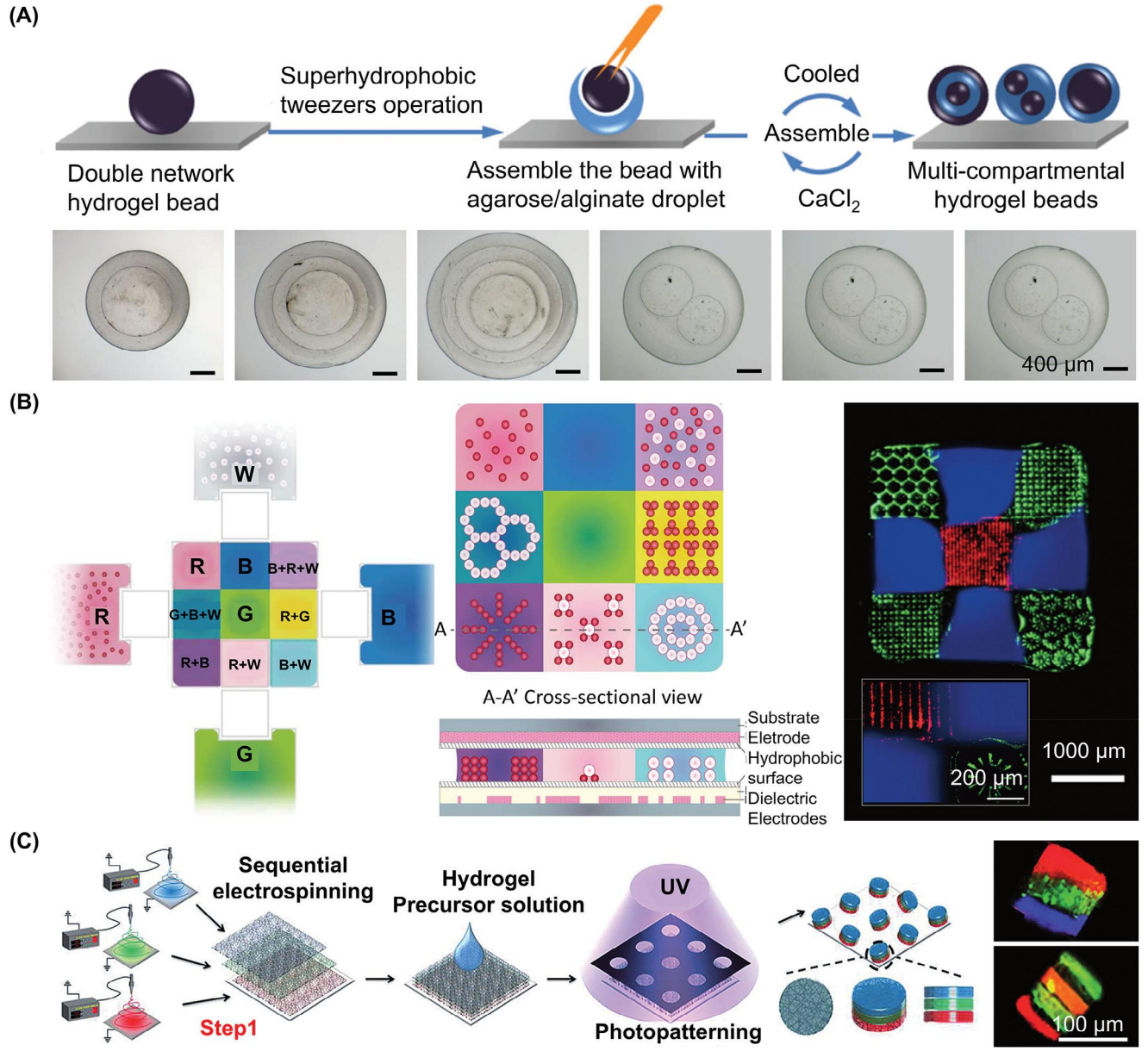

Figure 11. Preparation of AMs with other methods. A) Preparation of agarose/alginate double-network multicompartmental APs on a superhydrophobic surface. Adapted with permission.[83] Copyright 2014, Wiley-VCH. B) Fabrication of 3D complex architectures by two major electrical manipulations (electrowetting and dielectrophoresis) between two parallel plates of electromicrofluidic platform. Adapted with permission.[84] Copyright 2016, American Association for the Advancement of Science. C) Preparation of nonspherical hydrogel microparticles via combining electrospinning and photopatterning. Adapted with permission.[85] Copyright 2015, Wiley-VCH.

industrial mass production are limited by the template size and quantity. Similarly, although the template-based method is effective for fabricating AMs with shapes dictated by the mold, its production yield is inherently constrained by the limitations of the mold. Further study of other AM preparation techniques, such as flow lithography, is expected to combine lithography and template-based methods to solve the problem of low throughput.[6c]

To reduce the toxicity of the preparation process, preparation-friendly strategies such as 3D printing, EHD cojetting, and centrifuge-based and gas-based methods are required. A principal advantage of 3D printing is its capacity to form anisotropic microcarriers with exceptional design flexibility and structural complexity.[87] However, the current limitation of 3D printing is the relatively large feature sizes of the generated patterns. Significant advancements in printing precision have revealed the vast potential of anisotropic AM fabrication.

Furthermore, although recent studies have demonstrated notable progress in the EHD cojetting system, its inherent limitation in providing morphological versatility for AMs remains a significant challenge.[88] In comparison with other fabrication techniques, the microparticles produced by this method exhibit

inferior morphological characteristics and homogeneity. Although it can generate uniform microparticles, its size is typically larger and less controllable, presenting a notable limitation.

Centrifugation offers significant advantages, including a straightforward fabrication process and rapid operation. However, from a scalability standpoint, achieving continuous and high-throughput production remains challenging because of the complexities associated with controlling rotating microfluidic devices and integrating external instrumentation.[89] Gas-based strategies represent a relatively novel approach and are expected to attract increasing attention in the field owing to their numerous advantages including high throughput, oil-free operation, and surfactant-free conditions.[90] This approach can effectively address the limitations of other strategies; however, its reliance on surface tension for particle formation confines the resulting complexes to a microspherical morphology. Similarly, sputter coating presents several challenges. Despite the ease and speed of operation, the selectivity of materials is limited because numerous biocompatible materials are unsuitable for use.[91]

3. Applications of AMs

3.1. Multidrug Delivery

In drug delivery systems, the use of AMs for the encapsulation and delivery of multiple drugs has attracted increasing attention because of their unique benefits, including controlled release profiles,[92] potential for combination therapy,[93] enhanced efficacy,[94] and reduced side effects.[95] Ideally, these carriers should be able to release multiple drugs simultaneously in a controlled manner. To date, a range of AM-based drug carriers has been developed to achieve release functions. Common AMs used to load multidrug and enable their programmed release include Janus, core–shell, and multicore microparticles. However, polydisperse microparticles produced by emulsification provide limited control over the rate of polymer degradation and drug release.[33b] The production of intricate carriers requires precise flow control to generate complex emulsion templates, which limits the practical application of carriers. Although recent advances have introduced straightforward methods for creating complex emulsions from single emulsions through controlled phase separation, producing biocompatible multicompartment microcarriers based on a restricted range of materials useful for phase separation remains challenging.

Different materials can be prepared into AMs in microfluidic systems, thereby enabling precise control over the drug release kinetics through tailored material degradability. Sun et al.[96] proposed a flow-focusing microfluidic chip capable of producing various microparticle structures, including Janus-patchy, triple, quadruple, or core–shell types, from a mixed solution. The proportions of the two compartments in a particle can also be adjusted. Based on the phase transition of lipids from solid to liquid at physiological temperatures, the loaded drug is rapidly released and polymers undergo slow degradation in vivo, facilitating sustained drug release. This staged release mechanism is particularly beneficial for treatments requiring both rapid and slow drug release, such as targeted drug delivery and initial wound treatment. Moreover, the precise engineering of drug release rates can be achieved by utilizing the different responsiveness of polymers. Weaver et al.[97] reported complex liquid-based structures as dual-responsive drug-release models with high morphological control and uniformity. Each hemisphere of the AMs underwent stepwise disassembly, first triggered by pH changes and then by temperature stimulation (**Figure 12A**). The white hemisphere, which consisted of "conventional" spherical dodecane droplets, disintegrated swiftly at higher pH levels in the solution. This resulted in a thermally trapped 1-dodecanol hemisphere, which also decomposed quickly when the temperature of the solution was raised above the melting point of 1-dodecanol at basic pH. Growth factors can also be encapsulated into the AMs. Cho et al.[85] prepared AMs using hydrogel photopatterning and electrospinning (Figure 12B). Each compartment of the dual growth factor-loaded bicompartmental hydrogel microparticles was independent of the others and specifically released two different factors.

Concomitant drug therapy plays a pivotal role in enhancing the efficacy or reduces the side effects of drugs. However, the drug kinetics of individual constituents cannot be customized independently, which limits its extensive applications in the biological, chemical, and biomedical fields, such as confined reactions and controlled release. Therefore, independent encapsulation and synergistic release of diverse drugs are essential.[98] For example, a Janus shell embedded with thermoresponsive APs was fabricated using coextrusion minifluidic devices to achieve engineer thermoresponsive shell permeability for tunable release (Figure 12C).[99] At 25 °C, as a result of the swollen condition of the poly(nisopropylacrylamide) (PNIPAM) hydrogels in the Ca–SA hydrogel networks, their release behavior is similar to that of Ca–SA hydrogels lacking PNIPAM. Nevertheless, at 40 °C, the contraction of the PNIPAM APs increases the permeability, resulting in faster drug diffusion and more flexible synergistic release.

In addition to temperature, pH regulation can be employed to control drug release. Stimulating reactive carriers to release multiple drugs for synergistic combinatorial cancer therapy with reduced adverse reactions has been extensively studied. The pH-sensitive multicompartmental particles effectively and selectively released their payloads in acidic environments (Figure 12D). For example, acid-sensitive precursors have been substituted with PEGDA precursors to prepare drug carriers with pH-sensitivity. The drug release behavior from a compartment can be precisely adjusted by modifying the quantity of acid-sensitive precursors in the precursor solution.[100]

In biomedicine, the multidrug synergistic release of AMs has been extensively investigated for applications. SA AFs with multiple metal–organic framework (MOF) core encapsulations were used to improve tissue wound healing, allowing for highly controllable release by controlling the flow rates and orifice of the middle capillary (Figure 12E). The zinc- and copper–MOF–collagen AFs exhibited faster healing based on the antioxidation and antibiosis of controllably released zinc ions, copper ions, and vitamin ligands.[101]

Although multidrug release has demonstrated significant potential in various fields, there is room for improvement. For example, the capsule of two components in the corresponding zone without diffusion between the two compartments is a problem worth considering.[99] Furthermore, transformative advancements in artificial intelligence (AI) applications in biomedicine

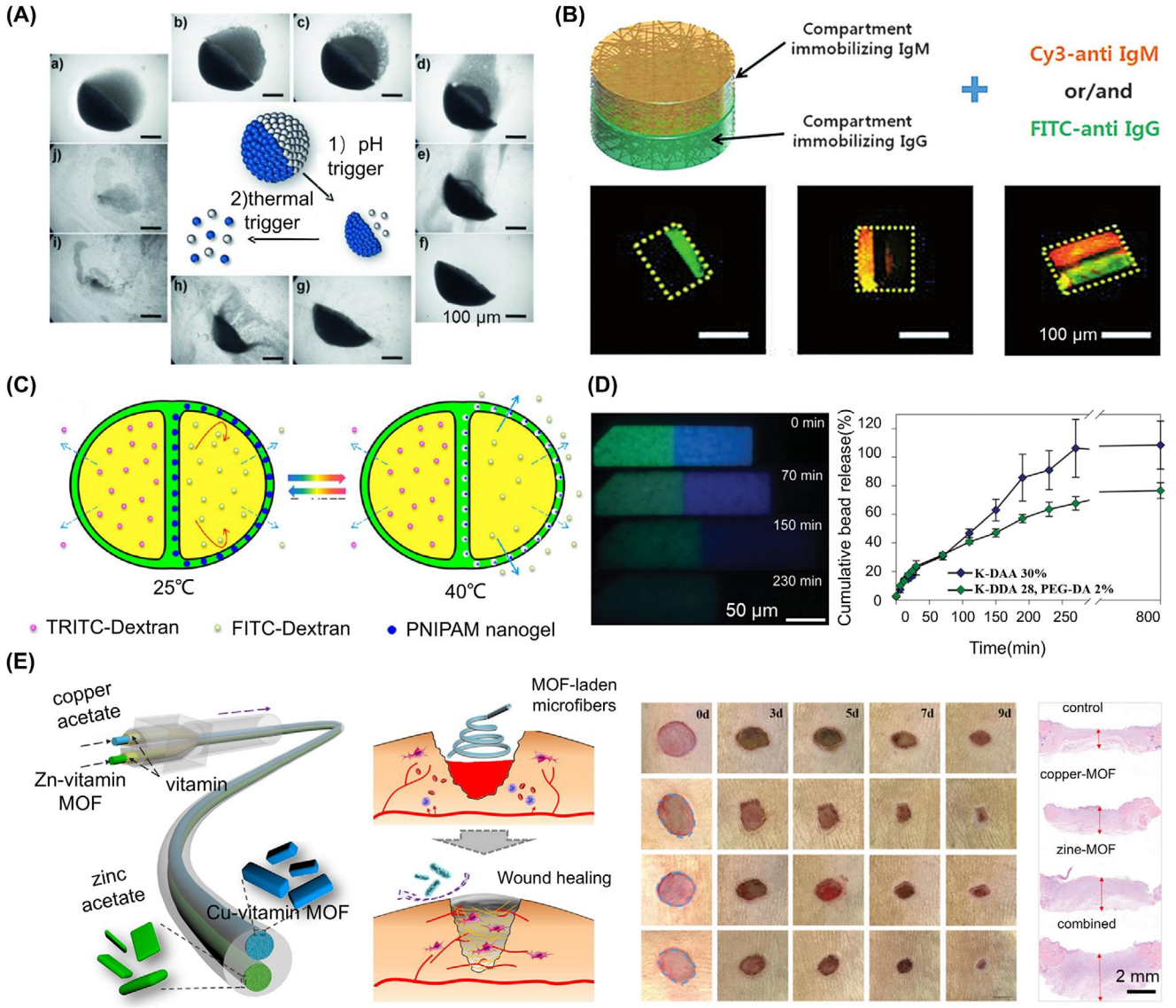

Figure 12. AMs for multidrug delivery. A) Dual-responsive drug-release models with pH and thermal triggers. Adapted with permission.[97] Copyright 2009, Wiley-VCH. B) APs formed by electrospinning and hydrogel photopatterning techniques for releasing two different growth factors with independent release kinetics. Adapted with permission.[85] Copyright 2015, Wiley-VCH. C) Permeability of Janus shell embedded with thermoresponsive nanogels controlled by temperature resulting in controlled release of drug. Adapted with permission.[99] Copyright 2016, American Chemical Society. D) Fluorescent beads release profiles of Janus particles with different ratios of acid-sensitive precursors compositions at pH 6.0. Adapted with permission.[100] Copyright 2016, Wiley-VCH. E) Vitamin MOF-laden microfibers with alginate shells and copper- or zinc–vitamin framework cores for wound healing. Adapted with permission.[101] Copyright 2018, Royal Society of Chemistry.

have occurred in recent years, particularly in drug delivery.[102] For example, powerful machine learning algorithms can optimize AM design parameters (e.g., shape, surface charge gradients, material biocompatibility, and targeting specificity) to enhance therapeutic efficiency.

3.2. Cell Coculture

In vivo, microenvironments are highly complex, consisting of anisotropic structures in which various cell types are organized in a structured manner, each being surrounded by a different extracellular matrix (ECM). Therefore, the AMs will enable the coassembly of diverse cell types within various ECMs, mirroring in vivo microenvironments. This capability allows the regulation of cellular behavior within an anisotropic microenvironment, thereby enhancing the potential for high-throughput in vitro screening platforms. Accurate imitation of anisotropy observed in vivo is critical for the development of in vitro artificial tissue models. The development of an anisotropic ECM structure for the cultivation of different cell types is essential to expand the potential applications of AMs,[103] including the biomimetic encapsulation and cultivation of defined cell populations in vivo-like microenvironments. However, current methodologies for the

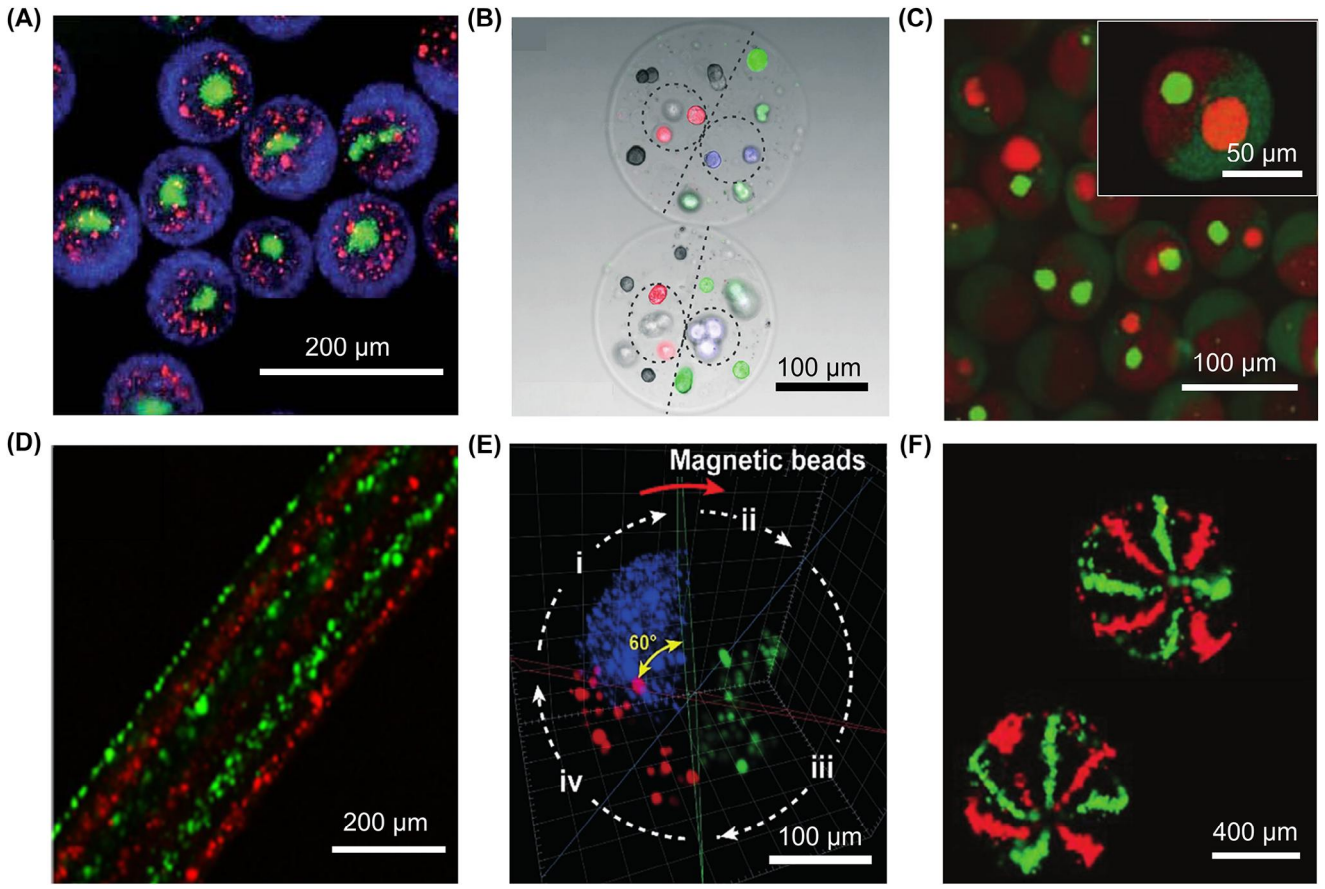

Figure 13. Cell coculture in AMs. A) Triple-layer particles prepared by one-step, multifluidic electrostatic spraying technique for cell encapsulation. Adapted with permission.[104] Copyright 2015, Royal Society of Chemistry. B) Single cells encased in different compartments of Janus microparticles. Adapted with permission.[105] Copyright 2017, Royal Society of Chemistry. C) Cells encapsulated in each compartment of four-compartmental core–shell microfibers. Adapted with permission.[13a] Copyright 2018, Wiley-VCH. D) Magnetic beads, fluorescent nanoparticles, and cells were coencased in APs to give the particles potential functions such as cell coding and rotational motion in response to magnet. Adapted with permission.[37] Copyright 2016, American Chemical Society. E) Four different types of cells were encapsulated in the desired compartments of APs for cell coculture. Adapted with permission.[106] Copyright 2020, Wiley-VCH. F) MCMs composed of up to eight compartments encase different cell types that are well separated from each other. Adapted with permission.[77] Copyright 2019, John Wiley and Sons.

formation of ECM microgels have not yet succeeded in producing anisotropic microparticles.

Hydrogel microparticles are widely used for cell encapsulation, culture, and transplantation. When transplanted, microparticles safeguard cells from environmental factors and the immune system while also facilitating the necessary mass transfer for cell survival and function. However, in many cases, cells are randomly encapsulated in microparticles because of their lack of spatial designability. Researchers can incorporate multiple materials into the anisotropic compartments or use different cell types. Therefore, another fascinating research area is exploring the potential of AMs in cell cocultures. The typical design of these AMs aims to facilitate the efficient and intelligent encapsulation of various cell types, allowing for effective control over the functionalities and characteristics of different compartments, which imparts unique properties to AMs. Microgels featuring independently regulated compartments capable of encapsulating cells within distinct hydrogel matrices would provide precise control over the pairing pathways of various cell types. For example, Lu et al.[104] produced AMs with devisable compartments by EHD cojetting method for cell coculture. This process is relatively simple and does not require surfactants, oils, or acids. **Figure 13A** demonstrated the capability of encapsulating distinct cell types within individual particles.

Microfluidic technology has been extensively developed for the fabrication of APs because it provided superior control over the morphology and complexity of the particles produced. Wu et al.[105] proposed a multiplex coaxial flow-focusing process to fabricate APs for cell cocultures. The produced APs featured a multicompartmental core–shell structure, with four different cell types encapsulated in their designated compartments of the SA APs and cocultured for seven days (Figure 13B). However, a significant limitation of microfluidic technology arises when it is necessary to encapsulate sensitive biological molecules within APs due to the reliance on oils and surfactants. Zhang et al.[13a] reported a microfluidic technology for inducing microgel formation on a chip, which could subsequently be extracted directly from the oil phase, thus effectively preventing extended temporal exposure of the AMs to oil. They proved that multicompartment microgels could be used first as a 3D matrix to pair single cells

(Figure 13C). Cocultivation of MSCs and human umbilical vein endothelial cells (HUVECs) within the same microenvironment created by Janus microgels facilitated the direct generation of an early marker for osteogenesis 8 days after encapsulation, indicating the osteogenic commitment of MSCs. This indicates that the interactions between MSCs and HUVECs may have a regulatory influence in determining the fate of stem cells, reflecting the feasibility of the current approach as a coculture platform for investigating intercellular communication. This highlights the extensive research on the development of AMs for designing cell coculture modules, which are essential in the fields of cell biology, stem cell therapy, and tissue engineering. Microfibers are used to load and coculture cells. Cheng et al.[37] reported a microfluidic method for continuously fabricating bioactive microfibers that could be utilized to create different tissue constructs for cell coculture (Figure 13D). This approach leveraged multiple laminar flows and a rapid cross-linking reaction of SA, enabling the generation of a series of cell-laden AFs with customizable morphological and structural features. To broaden more potential applications, Wu et al.[106] proposed a microfluidic technology for fabricating AMs based on a chip. They fabricated multiple ultracompartments to facilitate the coculture of a greater variety of cell types and incorporated additional functionalities such as magnetic beads and fluorescent nanoparticles (Figure 13E).

To date, a series of AMs have been produced using capillary array microfluidic devices that provided optimal control over the morphology and complexity of particles. Additionally, initiatives have been minimized the duration of exposure of cell-loaded AMs to adverse conditions, such as cytotoxicity, oils, surfactants, and UV irradiation, which often presented significant challenges. Therefore, for cell culture within AMs, developing a fabrication process that is straightforward and capable of high-throughput production is essential while operating under conditions devoid of oil and surfactants. Tang et al.[77] presented a one-step oil-free method utilizing gas-shearing to fabricate APs with up to eight distinct compartments (Figure 13F). The proposed gas-shearing strategy facilitated the production of APs containing various cell types, such as $HepG_2$ and HeLa cells within separate compartments. These APs, which contain eight distinct cell types that can be effectively isolated from one another, are particularly valuable for 3D cell cocultures. Moreover, previous methodologies for microparticle fabrication have not been successful in constructing such anisotropic microparticles.

3.3. Multifunctional Encoded Materials

With the emergence of the information age, the significance of materials for encoding information storage has increased. These materials have attracted considerable interest in various application areas, including computing, logistics, and medicine. Recent advancements in microbarcodes based on AMs have made significant progress owing to their application, flexibility, and ultrasmall size. For example, Stefaan et al. proposed an approach for encoding polymer microparticles.[42] The designed patterns were etched in fluorescently stained microparticles through spatially selective photobleaching and subsequently identified using confocal microscopy (**Figure 14A**). In addition to microparticles, they proposed the fabrication of digitally encoded fibers. They employed an electrospinning strategy to fabricate microscale fibers and encoded them using a photolithographic bleaching to obtain AFs (Figure 14B).[65] The introduction of digitally encoded microparticles can serve as a critical tool to combat the increasingly sophisticated drug counterfeiting. Encoded materials require trade-offs between scalability, encoding density, decoding, accuracy, and portability, which limit versatile information carriers and their widespread integration into industrial processes.

Therefore, a systematic multiscale design method was proposed to develop a powerful encoding technique for high-throughput preparation of encoded microparticles (Figure 14C).[48] This architecture demonstrates encoding capabilities that scale exponentially, features an exceptionally low rate of decoding false alarms, possesses the capacity to manipulate particles through the application of magnetic fields, and exhibits considerable insensitivity to variations in demanding fabrication parameters. In addition to its basic anticounterfeiting applications, this structure can significantly enhance the practical encoding capacity of multiplexed bioassays to unprecedented levels. PEGDA particles with unique coding and bioassay regions have been used to detect multiple microRNAs (miRNAs). One region contained an miRNA probe for miR-210, whereas the other region included a probe for miR-221.

Heterogeneous structural colors such as stripe colors are essential for camouflage and individual recognition.[107] To remotely control the change in structural colors, Zhao and co-workers designed structural color materials by rapidly self-assembling colloidal nanoparticles within capillaries (Figure 14D).[108] The dimensions and arrangement of the resultant structural color stripes can be accurately adjusted by modifying the parameters associated with self-assembly. NIR-light-responsive graphene hydrogels were integrated into a structural color stripe pattern, enabling self-reported and reversible bending behavior. Structural color stripe-patterned composite materials can be used in typical anticounterfeiting applications and have the potential to mimic structural colors in organisms, develop intelligent sensors and anticounterfeiting devices, and so on.

Most barcode preparation technologies rely on microfluidics and photolithography. However, these methods are often constrained by limitations in throughput and general applicability. Moreover, because of the fixed properties of molds, micromolding technologies restrict the morphologies and structures that can be created, rendering them unsuitable for barcode generation. To address these problems, a 3D dynamic micromolding method was proposed to fabricate novel photonic barcodes (Figure 14E).[109] This technology significantly enhanced throughput, allowing the simultaneous fabrication of numerous photonic barcodes. These barcodes could effectively and robustly perform high-throughput bioassays and had anticounterfeiting applications. To further improve the versatility of barcodes, Tang et al. proposed ten-faced memory microparticles with seven coding colors from three primary colors (Figure 14F).[110] The preparation process without organic chemical processes had a high throughput (>5000 microparticles per min) and was biofriendly. Because of their excellent biocompatibility, barcodes produced using these two methods can be applied in the food and

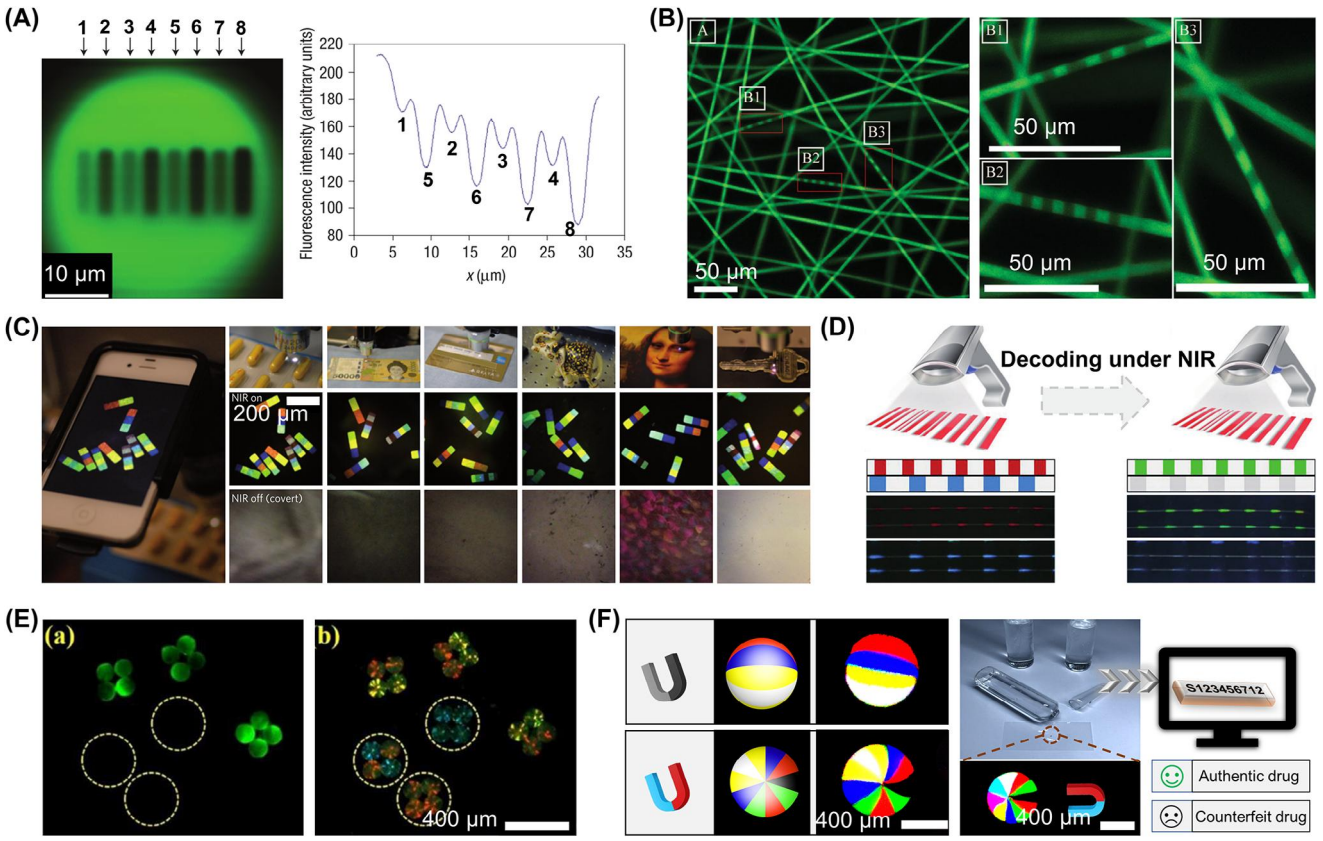

Figure 14. AMs for multifunctional encoding. A) Encoding microspheres by spatial selective photobleaching. Adapted with permission.[42] Copyright 2003, Springer Nature. B) Digitally encoded filaments to stop medicine counterfeiting. Adapted with permission.[65] Copyright 2010, Wiley-VCH. C) Encoded particles with a portable decoder applied in a range of complex substrates including pharmaceutical packaging, paper currency, credit cards, curved ceramic objects, reproduced artwork, and high-temperature-cast polystyrene. Adapted with permission.[48] Copyright 2014, Springer Nature. D) Heterogeneous structural color stripes applied in constructing intelligent sensors, and anticounterfeiting devices. Adapted with permission.[108] Copyright 2017, Wiley-VCH. E) Multicolored photonic barcodes for anticounterfeiting applications and multiplex bioassays. Adapted with permission.[109] Copyright 2018, Royal Society of Chemistry. F) Fabrication of biocompatible digitally color-tunable barcoding for food and pharmaceutical anticounterfeiting. Adapted with permission.[110] Copyright 2020, Wiley-VCH.

pharmaceutical fields, significantly improving the versatility of barcodes and information security. In the future, multifunctional encoded materials are expected to attract increasing interest, particularly in the fields of biomedical engineering and materials science.

3.4. Biomimetic Multienzyme Cascade Tandem Reaction System

Enzymes serve as powerful biocatalysts that facilitate all essential biological processes in living organisms.[111] Various enzymes have distinct roles separately and simultaneously in this process. Typically, many common enzymatic reactions involve single-enzyme catalysis. However, complex reactions often require two or more enzymes. Therefore, the development of multicompartmental systems designed to carry out various biochemical reactions in one space, such as in living cellular systems, has attracted considerable interest.[112] In the context of enzyme carrier applications, the prepared AMs must be biocompatible and have a soft interface with biological systems. An effective fabrication strategy must be able to control sizes and morphologies of the multienzyme cascade tandem reaction system, such as the precise operational capability of the type, number, and spatial arrangement of the laden enzymes to enhance the efficiency of the cascade reaction.[113]

Microfluidic platforms are often employed to fabricate APs for multienzyme cascade reactions.[114] Chen and co-workers presented a design for multicompartmental hydrogel particles using microfluidic strategies, where different enzymes enabled spatial immobilization within separate domains, facilitating engineered tandem reactions (**Figure 15A**).[17b] The dense encapsulation of distinct compartments with distinct pH microenvironments in APs allowed for the effective transport of reactants, ensuring efficient product generation. They also revealed that hydrogel APs could facilitate a glucose-triggered, incompatible, and multistep tandem reaction in a single vessel when partitioned and loaded with glucose oxidase and magnetic nanoparticles. Zhao and co-workers proposed a multienzyme system with the required characteristics: hollow hydrogel microcapsules with flexible and mobile enzymatically reversed opal particle encapsulation (Figure 15B).[115] They demonstrated that this system, containing alcohol catalase and

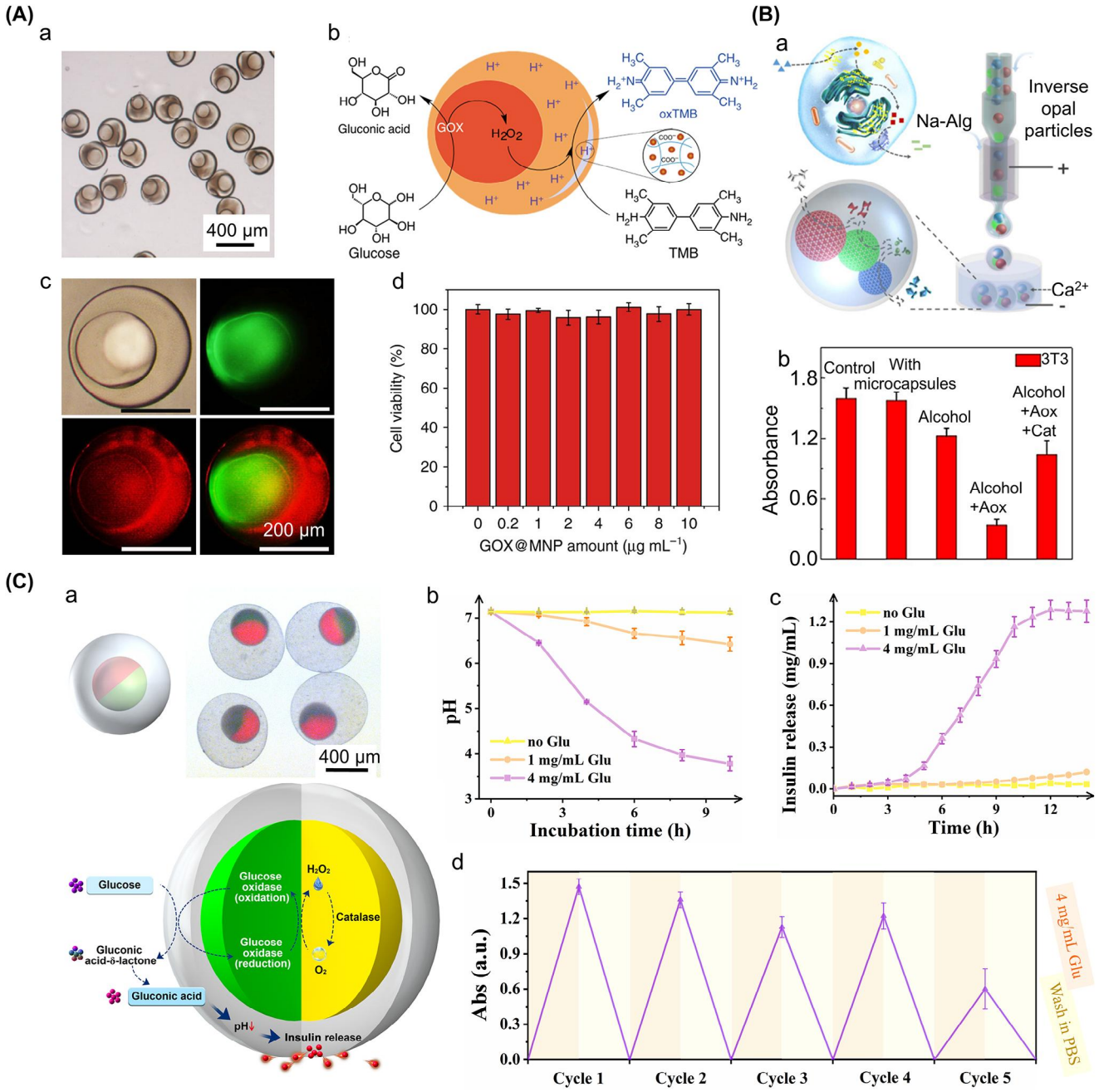

Figure 15. Biomimetic multienzyme cascade tandem reaction system in AMs. A) (a,b) AMs prepared by the microfluidic device could process a glucose-triggered, incompatible, multistep tandem reaction in one pot when partitioned loading glucose oxidase and magnetic nanoparticles. (c) Confocal image of multicompartmental hydrogel particles. (d) Cell viability of HeLa cells. Adapted with permission.[17b] Copyright 2017, Springer Nature. B) (a) Multienzyme system with flexible and mobile enzymatic inverse opal microparticle. (b) Cell viability in multienzyme microcapsule system. Adapted with permission.[115] Copyright 2018, American Association for the Advancement of Science. C) (a) Microscopy images of two mangosteen-like microparticles. Glucose oxidase and catalase were separately encapsulated in two compartments. (b) pH changes in microparticles with time in a glucose solution. (c) Release of insulin in the microparticle. (d) DAP absorbance of microparticles in glucose solution (for five subsequent cycles). Adapted with permission.[116] Copyright 2022, Elsevier B.V.

oxidase, could function as a cascade biocatalyst to reduce alcohol concentrations in the medium, providing a prophylactic and alternative antidote for alcohol intoxication. Recently, core–shell APs were developed using gas-shearing strategies to enable the precise control of enzymatic cascade reactions aimed at achieving insulin release (Figure 15C).[116] Glucose catalase and oxidase were individually loaded within distinct compartments of the SA cores, whereas insulin was encapsulated in the chitosan shell. The core–shell APs, served as an artificial pancreatic β-beta cell, capable of releasing insulin

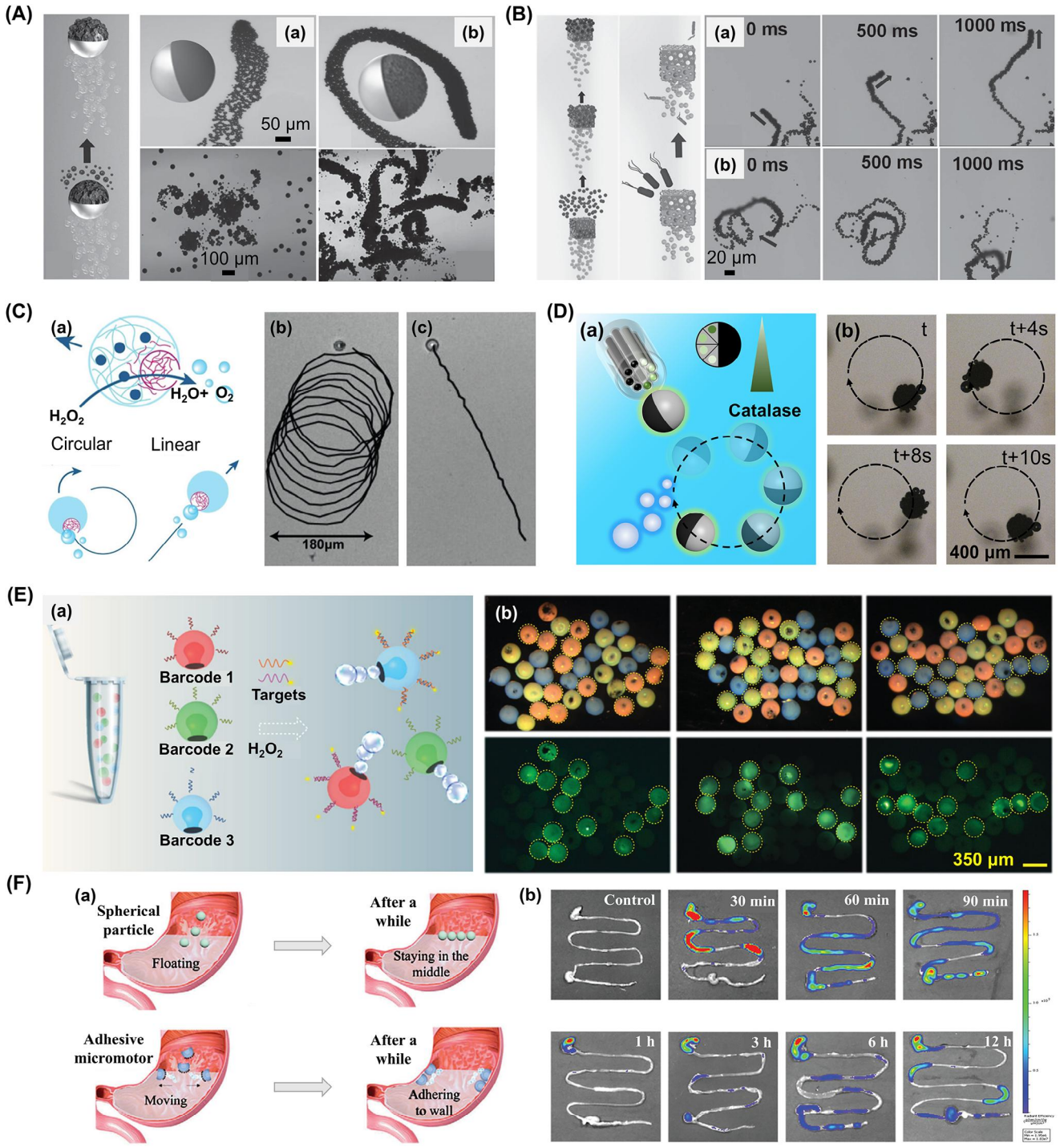

Figure 16. Application of AMs as micromotors. A) (a) The dark hemisphere (right) represents the activated carbon, while the gray area (left) corresponds to the catalytic Pt. The activated carbon-based Janus particle micromotors (b) have a higher bubble production rate and faster movement speed than the common polystyrene/Pt Janus micromotors. Adapted with permission.[122] Copyright 2015, Wiley-VCH. B) Combining silver ions (Ag^+) and chemical warfare agents into an aluminosilicate zeolite framework in micromotors could carry the curved, circular, and self-rotating motion. Adapted with permission.[123] Copyright 2015, Wiley-VCH. C) APs composed of incompatible two-phase hydrogel solutions can easily complete sustained circular or linear motion. Adapted with permission.[14b] Copyright 2018, Wiley-VCH. D) Controllable circular motion of Janus hydrogel microparticles with gradient multicompartmental structures under a magnetic field. Adapted with permission.[124] Copyright 2021, Elsevier B.V. E) (a) Stomatocyte colloidal crystal cluster micromotors for multiplex detection. (b) Three types of micromotors incubate with the target DNAs. Adapted with permission.[125] Copyright 2020, Oxford University Press. F) Suction-cup-like micromotors show stronger adhesion and retention rate than traditional spherical particles. Adapted with permission.[126] Copyright 2022, John Wiley and Sons.

in response to increased glucose concentration. The cascade reactions of the two enzymes in the APs lasted for five cycles, demonstrating that the artificial cells maintained sufficient functionality to facilitate the enzymatic reactions. To provide a novel tool for performing enzymatic cascade reactions, Kamperman et al. prepared the Janus microparticles using "in-air microfluidics" to combine liquid microjets in midair, resulting in production rates of Janus microparticles that were several orders of magnitude faster (≈mL min^{-1}) compared to chip-based microfluidics.[35] The enzymes glucose oxidase and horseradish peroxidase were encapsulated in the APs. After a series of catalytic reactions, the colorimetric shift from colorless to brown in the precipitation of poly(3,3′-diaminobenzidine) indicated the successful occurrence of the enzymatic cascade reaction. The application of AMs to multienzyme cascade tandem reactions provide an excellent and convenient platform for simulating the complex biocatalytic and biomimetic functions of organelles or organs.

3.5. Micromotors

Inspired by natural microbial swimming, AMs have been used as micromotors to emulate the functions of these distinctive natural systems across various morphologies, in addition to the aforementioned applications. They primarily existed like helical microfibers, rolled-up microtubes, and Janus particles, which have been engineered for a variety of applications including environmental simulation,[117] biosensing,[118] drug delivery,[119] and cell manipulation.[120] Various strategies have been employed to fabricate micromotors, including electrochemical synthesis, 3D printing, and microfluidic technology.[121] Researchers have focused on enhancing the locomotion capabilities of micromotors from simple to complex. Singh and co-workers developed self-propelled Janus-particle micromotors containing activated carbon that exhibited effective movement in environmental matrices and effectively removed a wide range of organic and inorganic pollutants (**Figure 16A**).[122] They demonstrated enhanced locomotion capabilities by controlling fuel concentration. Instead of a smooth catalytic surface, the microporous structure of the catalytic platinum (Pt) layer leads to a higher bubble production rate and a greater water purification efficiency in considerably shorter time frames compared to static activated carbon particles. Wang and co-workers developed micromotors capable of effectively and rapidly eliminating chemical and biological threats.[123] Specifically, silver ions were added to the framework of aluminosilicate zeolites, resulting in several advantageous properties, including solid binding to chemical warfare agents, efficient degradation, and improved antibacterial activity. As illustrated in Figure 16B, a long, high-density tail of oxygen microbubbles was produced and released from the sputtered silver surface, leading to effective bubble propulsion and improved fluid movement. These micromotors are capable of curved, circular, and self-rotating motions; however, these movements are random rather than controllable. Moreover, most designs rely on top-down fabrication methods for constructing inorganic motors, which are labor-intensive and unsuitable for biomedical applications. To expand their potential for biomedical applications, as shown in Figure 16C, Wilson et al. developed a high-throughput strategy for the fabrication of asymmetric AMs with autonomic movement. Asymmetric, aqueous, two-phase-separating droplets were generated using a microfluidic chip containing dextran and PEGDA with the biocatalyst positioned in the PEGDA phase.[14b] The motor operated through the enzyme-catalyzed breakdown of the fuel. The velocity of the motors was affected by the surface roughness of the PEGDA following dextran diffusion, and this velocity could be modulated by employing dextran with a greater molecular weight. The roughness of the surface facilitated the attachment of oxygen bubbles, resulting in an increased motor speed. Bubble pinning was consistently produced at the exact location, leading to sustained linear or circular motion. To ensure biocompatibility, SA APs authorized by the United States Food and Drug Administration were fabricated via gas-shearing. Additionally, biocompatible iron oxide (Fe_3O_4) nanoparticles or biocatalytic catalase have been utilized to generate propulsion for the micromotors (Figure 16D).[124]

Monodisperse nanoparticles can be assembled into colloidal crystal clusters through rapid solvent extraction within microfluidics. The aggregated particles resembled stomatocytes or exhibited a suction-cup-like morphology. These were then used as templates for hydrogel replication, after which the nanoparticles were removed. Hydrogel micromotors can be prepared by loading Pt or Fe_3O_4 into cavities. Their capacity for autonomous movement facilitates the capture of more targets, opening new avenues for sensing and detection applications (Figure 16E).[125] The self-propelling nature of micromotors, along with their unique suction cup-like and porous structures, make them ideal vehicles for drug delivery in the gastric environment. Magnesium is loaded onto the surface of the particles, resulting in the continuous generation of hydrogen bubbles in the gastric juice, which enable spontaneous movement. Micromotors can effectively adsorb onto gastric ulcers and release drugs. The results indicate that they exhibit stronger adhesion and retention rates than traditional spherical particles and efficient therapeutic effects in the treatment of gastric ulcers (Figure 16F).[126]

However, most of the aforementioned technologies for fabricating micromotors are costly and/or labor-intensive. Achieving high throughput and uniform quality in the fabrication of these micromotors has always been a challenge. The preparation process and resulting micromotors often lack biocompatibility. Complex manufacturing technologies are necessary for asymmetric surface modifications, which are highly time-intensive. For biomedical applications, the prepared micromotors must be biodegradable, biocompatible, and have soft interfaces.

3.6. Other Applications

Apart from these functions, AMs can also be used in multitarget detection or biosensing, multimodal bioimaging,[127] and as cell receptor activators.[128] Preliminary studies have indicated the possibility of integrating cell targeting capabilities with surface-enhanced sensing functionality into individual Janus microparticles. In other words, AMs (mainly Janus particles) can directly influence the spatial arrangement of signaling proteins and

Table 1. Advantages and disadvantages of methods for fabricating AMs.

Method	Advantages	Disadvantages
Microfluidics strategy	• High controllability of droplet diameter • Good monodispersity • Wide selection of materials	• The inevitable use of oils, photoinitiators, crosslinkers, surfactants, and UV-irradiation
Lithography	• Great control of the geometry • Good monodispersity	• Low complexity of internal or external features • Low throughput
3D printing	• Highly designable and complex	• Low accuracy
Electrohydrodynamic (EHD) cojetting	• High throughput • Wide particle size range	• Poor morphology and uniformity • Small-scale controllability
Centrifugation	• Easy to operate • Good monodispersity	• Low throughput
Gas-based method	• High throughput • Oil-free; surfactant-free	• Low stability
Templating method	• High controllability of particle diameter • Good monodispersity	• Low throughput

receptors on phagosomes inside living cells. Yu et al.[129] provided empirical evidence that Dectin-1 and Toll-like receptor 2 must be positioned within nanoscale proximity to phagosomes to elicit synergistic antifungal responses in macrophages. This methodology elucidated the interactions between receptors and their signaling pathways through physical manipulation and was extendable to other phagocytic receptor extendable innate immune cells.

4. Conclusions

This review highlights how the anisotropy in microcarriers endows them with unique properties. AMs have developed into a compelling and novel category of particulate carriers composed of various building blocks with different physical, chemical, and material properties. Numerous strategies have been developed to fabricate AMs from anisotropic materials. The appropriate preparation method for AMs can be determined based on the application requirements such as resolution, throughput, and biocompatibility (**Table 1**). Among them, as an emerging strategy, the advantages of 3D printing are prominent. An overview of the advantages and disadvantages of each light-based 3D printing modality is presented in **Table 2**. Geometrically complex structures can be easily fabricated using 3D printing. However, fabricating microcarriers at the micrometer scale using 3D bioprinting is more challenging than using other methods, particularly for AMs. This emerging 3D volumetric printing method may facilitate the production of smaller AMs with multiple hydrogel preconstructions. Although these methods have distinct advantages and disadvantages, they can be complemented by a combination of two or more. For instance, combining a gas-based method with electrospraying is expected to yield uniform microparticles with smaller sizes.

The versatile and flexible preparation of designable and complex AM structures can further promote the development of various fields. This surface and structural anisotropy enables integration of multiple functions into a single microparticle. This, in turn, facilitates a wide variety of novel applications such as

Table 2. The advantages and disadvantages of each 3D printing modality.

Method	Advantages	Disadvantages
Inkjet printing	• High resolution • Suitable for multimaterial printing	• Difficult to build larger structures • Limited to low viscosity materials • Limited structural complexity
Extrusion printing	• Fast print time for small structures • Suitable for multimaterial printing	• Slow print time for larger structures • Limited to low viscosity materials • Limited resolution • Extrusion pressure reduces cell viability
Laser-based printing	• High resolution	• Not suitable for multimaterial printing • Not suitable for cell printing
DLP-based printing	• High resolution • Rapid printing time • Complex structures can be easily printed	• Difficult to print very soft constructs • Not suitable for opaque materials (severely limiting penetration and resolution)
3D volumetric printing	• Fast print time for larger structures • Suitable for printing very soft constructs • Complex structures can be easily printed	• Not suitable for opaque materials (severely limiting penetration and resolution)

enzyme cascades, multidrug delivery, and exploration of cell–cell interactions. Compartments with multiple properties, such as magnetic and fluorescent nanoparticles, drugs, and biomolecules, can be integrated to form AMs that facilitate simultaneous imaging, diagnosis, and therapy. The examples described in this review offer only a glimpse into the extensive range of novel applications made possible by AMs. Nonetheless, these examples illustrate the significant potential of this novel particulate system for biomedical innovation. However, further efforts are needed to explore the fundamental aspects of AM research, including the interaction of AMs with biological systems and their combination with other emerging technologies, such as AI. In the future, multicompartment microparticles encasing bioactive substances, microorganisms, and phased release of drugs will attract significant attention.

Supporting Information

Supporting Information is available from the Wiley Online Library or from the author.

Acknowledgements

Y.H., L.X., and W.M. contributed equally to this work. This work was supported by the National Natural Science Foundation of China (NSFC) Program (No. 32201183), Science and Technology Program of Guangzhou (SL2022A04J00774), Opening Project of Guangdong Province and NMPA & State Key Laboratory (J24413003), Guangdong Basic and Applied Basic Research Foundation (2021A1515220174), and the Administration of Traditional Chinese Medicine of Guangdong Province (20241183). [Correction added on March 24, 2025, after first online publication: Figure 12 has been replaced.]

Conflict of Interest

The authors declare no conflict of interest.

Keywords

anisotropic microcarriers, cell coculture, multidrug delivery, multifunction coding

Received: November 2, 2024
Revised: March 8, 2025
Published online: March 21, 2025

[1] a) W. H. Tan, S. Takeuchi, *Adv. Mater.* **2007**, *19*, 2696; b) D. Steinhilber, T. Rossow, S. Wedepohl, F. Paulus, S. Seiffert, R. Haag, *Angew. Chem.* **2013**, *52*, 13538; c) X. Zhao, S. Liu, L. Yildirimer, H. Zhao, R. Ding, H. Wang, W. Cui, D. Weitz, *Adv. Funct. Mater.* **2016**, *26*, 2809; d) A. S. Mao, J. W. Shin, S. Utech, H. Wang, O. Uzun, W. Li, M. Cooper, Y. Hu, L. Zhang, D. A. Weitz, D. J. Mooney, *Nat. Mater.* **2017**, *16*, 236; e) Y. Xu, H. Wang, C. Luan, F. Fu, B. Chen, H. Liu, Y. Zhao, *Adv. Funct. Mater.* **2017**, *28*, 1704458; f) L. Y. Xuan, Y. Y. Hou, L. Liang, J. L. Wu, K. Fan, L. M. Lian, J. H. Qiu, Y. L. Miao, H. Ravanbakhsh, M. E. Xu, G. S. Tang, *Nano-Micro Lett.* **2024**, *16*, 218.

[2] a) K. H. Roh, D. C. Martin, J. Lahann, *Nat. Mater.* **2005**, *4*, 759; b) F. Sciortino, A. Giacometti, G. Pastore, *Phys. Rev. Lett.* **2009**, *103*, 237801; c) F. Wurm, A. F. Kilbinger, *Angew. Chem., Int. Ed.* **2009**, *48*, 8412; d) A. Walther, A. H. Muller, *Chem. Rev.* **2013**, *113*, 5194; e) J. Zhang, B. A. Grzybowski, S. Granick, *Langmuir* **2017**, *33*, 6964; f) B. Z. Shutong Qian, J. Mao, Z. Liu, Q. Zhao, B. Lu, X. Mao, L. Zhang, L. Cheng, Y. Zhang, W. Cui, X. Sun, *Biomed. Technol.* **2023**, *2*, 58.

[3] A. Ajdari, *Science* **2007**, *317*, 466.

[4] a) S. Li, Y. Yang, S. Wang, Y. Gao, Z. Song, L. Chen, Z. Chen, *Exploration* **2022**, *2*, 20210223; b) J. T. Lovegrove, B. Kent, S. Forster, C. J. Garvey, M. H. Stenzel, *Exploration* **2023**, *3*, 20220075.

[5] a) Y. Zhao, H. Gu, Z. Xie, H. C. Shum, B. Wang, Z. Gu, *J. Am. Chem. Soc.* **2013**, *135*, 54; b) S. N. Yin, S. Yang, C. F. Wang, S. Chen, *J. Am. Chem. Soc.* **2016**, *138*, 566; c) D. Q. Huang, Z. H. Wu, J. Wang, J. L. Wang, Y. J. Zhao, *Adv. Sci.* **2024**, *11*, 2406573; d) X. M. Jia, W. Y. Liu, Y. J. Ai, S. Cheung, W. T. Hu, Y. Wang, X. L. Shi, J. Zhou, Z. Zhang, Q. L. Liang, *Adv. Mater.* **2024**, *36*, 2404071.

[6] a) D. C. Pregibon, M. Toner, P. S. Doyle, *Science* **2007**, *315*, 1393; b) A. X. Lu, H. Oh, J. L. Terrell, W. E. Bentley, S. R. Raghavan, *Chem. Sci.* **2017**, *8*, 6893; c) C. C. Zhou, Y. W. Cao, C. X. Liu, W. L. Guo, *Mater. Today* **2023**, *67*, 178; d) R. Feng, F. Song, Y. D. Zhang, X. L. Wang, Y. Z. Wang, *Nat. Commun.* **2022**, *13*, 3078.

[7] a) J. Lee, J. Kim, *Chem. Mater.* **2012**, *24*, 2817; b) K. Maeda, H. Onoe, M. Takinoue, S. Takeuchi, *Adv. Mater.* **2012**, *24*, 1340.

[8] a) H. Zhao, Y. Chen, L. Shao, M. Xie, J. Nie, J. Qiu, P. Zhao, H. Ramezani, J. Fu, H. Ouyang, Y. He, *Small* **2018**, *14*, 1802630; b) J. Xu, S. Li, W. Lan, G. Luo, *Langmuir* **2008**, *24*, 11287; c) Z. N. Wu, Y. J. Zheng, J. M. Lin, G. W. Xing, T. Z. Xie, Y. N. Lin, J. X. Lin, L. Lin, *Chem. Eng. J.* **2024**, *502*, 158038.

[9] a) Y. Shang, Z. Chen, Z. Zhang, Y. Yang, Y. Zhao, *Bio-Des. Manuf.* **2020**, *3*, 266; b) M. Gil, S. Moon, J. Yoon, S. Rhamani, J.-W. Shin, K. J. Lee, J. Lahann, *Adv. Sci.* **2018**, *5*, 1800024.

[10] a) J. Xue, T. Wu, Y. Dai, Y. Xia, *Chem. Rev.* **2019**, *119*, 5298; b) Y. X. Cao, J. Y. Tan, H. R. Zhao, T. Deng, Y. X. Hu, J. H. Zeng, J. W. Li, Y. F. Cheng, J. Y. Tang, Z. W. Hu, K. E. Hu, B. Xu, Z. T. Wang, Y. J. Wu, P. E. Lobie, S. H. Ma, *Nat. Commun.* **2022**, *13*, 7463; c) A. C. Daly, M. D. Davidson, J. A. Burdick, *Nat. Commun.* **2021**, *12*, 753.

[11] a) C. H. Choi, S. M. Kang, S. H. Jin, H. Yi, C. S. Lee, *Langmuir* **2015**, *31*, 1328; b) C. H. Choi, J. Lee, K. Yoon, A. Tripathi, H. A. Stone, D. A. Weitz, C. S. Lee, *Angew. Chem.* **2010**, *49*, 7748; c) H. U. Kim, Y. H. Roh, S. J. Mun, K. W. Bong, *ACS Appl. Mater. Interfaces* **2020**, *12*, 53318; d) S. G. Jeong, Y. Choi, J. O. Nam, C. S. Lee, C. H. Choi, *J. Colloid Interface Sci.* **2021**, *582*, 1012.

[12] a) M. D. McConnell, M. J. Kraeutler, S. Yang, R. J. Composto, *Nano Lett.* **2010**, *10*, 603; b) S. Y. Lee, J. Choi, J. R. Jeong, J. H. Shin, S. H. Kim, *Adv. Mater.* **2017**, *29*, 1605450; c) W. Wu, Y. H. Xia, Y. Huang, W. Y. Wei, X. P. Wu, R. Tu, T. W. Chen, H. L. Dai, *Adv. Funct. Mater.* **2024**, *34*, 202410389.

[13] a) L. Zhang, K. Chen, H. Zhang, B. Pang, C. H. Choi, A. S. Mao, H. Liao, S. Utech, D. J. Mooney, H. Wang, D. A. Weitz, *Small* **2018**, *14*, 1702955; b) Y. Cheng, F. Zheng, J. Lu, L. Shang, Z. Xie, Y. Zhao, Y. Chen, Z. Gu, *Adv. Mater.* **2014**, *26*, 5184.

[14] a) H. Wang, M. Pumera, *Chem. Rev.* **2015**, *115*, 8704; b) S. Keller, S. P. Teora, G. X. Hu, M. Nijemeisland, D. A. Wilson, *Angew. Chem.* **2018**, *57*, 9814.

[15] a) T. G. Wang, A. V. Anikumar, I. Lacik, Google Patents, **1999**, 6001312; b) Y. Zhang, C.-F. Wang, L. Chen, S. Chen, A. J. Ryan, *Adv. Funct. Mater.* **2015**, *25*, 7253.

[16] a) Y. Qi, L. Chu, W. Niu, B. Tang, S. Wu, W. Ma, S. Zhang, *Adv. Funct. Mater.* **2019**, *29*, 1903743; b) D. H. Choi, R. Subbiah, I. H. Kim, D. K. Han, K. Park, *Small* **2013**, *9*, 3468; c) F. He, W. Wang, X. H. He, X. L. Yang, M. Li, R. Xie, X. J. Ju, Z. Liu, L. Y. Chu, *ACS. Appl. Mater.* **2016**, *8*, 8743.

[17] a) Z. Z. Huan Wang, Y. Liu, C. Shao, F. Bian, Y. Zhao, *Sci. Adv.* **2018**, *4*, 2816; b) H. Tan, S. Guo, N. D. Dinh, R. Luo, L. Jin, C. H. Chen, *Nat. Commun.* **2017**, *8*, 663.
[18] a) S. Yoshida, M. Takinoue, H. Onoe, *Adv. Healthcare Mater.* **2017**, *6*, 1601463; b) D. H. Kang, H. S. Jung, N. Ahn, S. M. Yang, S. Seo, K. Y. Suh, P. S. Chang, N. L. Jeon, J. Kim, K. Kim, *ACS Appl. Mater.* **2014**, *6*, 10631.
[19] a) E. Kang, G. S. Jeong, Y. Y. Choi, K. H. Lee, A. Khademhosseini, S. H. Lee, *Nat. Mater.* **2011**, *10*, 877; b) Q. Guo, Y. Wang, C. Chen, D. Wei, J. Fu, H. Xu, H. Gu, *Small* **2020**, *16*, 1907521.
[20] a) A. Pal, A. Gope, A. Sengupta, *Adv. Colloid Interface Sci.* **2023**, *314*, 102870; b) T. Zhang, D. Lyu, W. Xu, X. Feng, R. Ni, Y. Wang, *Nat. Commun.* **2023**, *14*, 8494.
[21] a) L. Cai, F. Bian, H. Chen, J. Guo, Y. Wang, Y. Zhao, *Chem.* **2021**, *7*, 93; b) J. P. Agusil, M. I. Arjona, M. Duch, N. Fusté, J. A. Plaza, *Small* **2020**, *16*, 2004691.
[22] A. Dasgupta, T. Sun, R. Palomba, E. Rama, Y. Z. Zhang, C. Power, D. Moeckel, M. J. Liu, A. Sarode, M. Weiler, A. Motta, C. Porte, Z. Magnuska, A. S. Elshafei, R. Barmin, A. Graham, A. McClelland, D. Rommel, E. Stickeler, F. Kiessling, R. M. Pallares, L. De Laporte, P. Decuzzi, N. McDannold, S. Mitragotri, T. Lammers, *Proc. Natl. Acad. Sci. USA* **2023**, *120*, 2218847120.
[23] Z. C. Ding, Z. M. Liang, X. Rong, X. X. Fu, J. X. Fan, Y. H. Lai, Y. R. Cai, C. Huang, L. L. Li, G. S. Tang, Z. Y. Luo, Z. K. Zhou, *Small* **2024**, *20*, 2403753.
[24] a) M. Lama, F. M. Fernandes, A. Marcellan, J. Peltzer, M. Trouillas, S. Banzet, M. Grosbot, C. Sanchez, M. M. Giraud-Guille, J. j. Lataillade, *Small* **2020**, *16*, 1902224; b) N. Kapate, J. R. Clegg, S. Mitragotri, *Adv. Drug Delivery Rev.* **2021**, *177*, 113807; c) S. Tao, B. Lin, H. Zhou, S. Sha, X. Hao, X. Wang, J. Chen, Y. Zhang, J. Pan, J. Xu, *Nat. Commun.* **2023**, *14*, 5575; d) J. B. Kim, S. Y. Lee, N. G. Min, S. Y. Lee, S. H. Kim, *Adv. Mater.* **2020**, *32*, 2001384; e) J. Cho, J. Cho, H. Kim, M. Lim, H. Jo, H. Kim, S.-J. Min, H. Rhee, J. W. Kim, *Green Chem.* **2018**, *20*, 2840; f) Y. Song, X. Wan, S. Wang, *Acc. Mater. Res.* **2023**, *4*, 1033; g) Y. Duan, X. Zhao, M. Sun, H. Hao, *Ind. Eng. Chem. Res.* **2021**, *60*, 1071.
[25] Y. Shi, J. Gu, C. Zhang, R. Mi, Z. Ke, M. Xie, W. Jin, C. Shao, Y. He, J. Shi, *Small* **2024**, *20*, 2403835.
[26] S. Yang, F. Wang, H. Han, H. A. Santos, Y. Zhang, H. Zhang, J. Wei, Z. Cai, *Biomed. Technol.* **2023**, *2*, 31.
[27] H. Zhang, J. K. Nunes, S. E. A. Gratton, K. P. Herlihy, P. D. Pohlhaus, J. M. DeSimone, *New J. Phys.* **2009**, *11*, 075018.
[28] a) Y. H. Choi, S. S. Lee, D. M. Lee, H. S. Jeong, S. H. Kim, *Small* **2019**, *16*, 1903812; b) H. T. Liu, H. Wang, W. B. Wei, H. Liu, L. Jiang, J. H. Qin, *Small* **2018**, *14*, 1801095.
[29] a) I. Mirza, S. Saha, *ACS Appl. Bio Mater.* **2020**, *3*, 8241; b) H. Xia, J. Li, J. Man, L. Man, S. Zhang, J. Li, *Mater. Today Commun.* **2021**, *29*, 102740.
[30] a) T. Nisisako, T. Torii, T. Higuchi, *Chem. Eng. J.* **2004**, *101*, 23; b) S.-H. Kim, S.-J. Jeon, W. C. Jeong, H. S. Park, S.-M. Yang, *Adv. Mater.* **2008**, *20*, 4129.
[31] C. H. Choi, D. A. Weitz, C. S. Lee, *Adv. Mater.* **2013**, *25*, 2536.
[32] N. G. Min, M. Ku, J. Yang, S.-H. Kim, *Chem. Mater.* **2016**, *28*, 1430.
[33] a) L. Y. Chu, A. S. Utada, R. K. Shah, J. W. Kim, D. A. Weitz, *Angew. Chem.* **2007**, *46*, 8970; b) W. Wang, R. Xie, X. J. Ju, T. Luo, L. Liu, D. A. Weitz, L. Y. Chu, *Lab Chip* **2011**, *11*, 1587.
[34] Z. Yu, C. F. Wang, L. Ling, L. Chen, S. Chen, *Angew. Chem.* **2012**, *51*, 2375.
[35] T. Kamperman, V. D. Trikalitis, M. Karperien, C. W. Visser, J. Leijten, *ACS Appl. Mater.* **2018**, *10*, 23433.
[36] a) X. Hou, Y. S. Zhang, G. T.-d. Santiago, M. M. Alvarez, J. Ribas, S. J. Jonas, P. S. Weiss, A. M. Andrews, J. Aizenberg, A. Khademhosseini, *Nat. Rev. Mater.* **2017**, *2*, 17016; b) L. Shang, Y. Yu, Y. Liu, Z. Chen, T. Kong, Y. Zhao, *ACS Nano* **2019**, *13*, 2749; c) C. Chávez-Madero, M. D. de León-Derby, M. Samandari, C. F. Ceballos-González, E. J. Bolívar-Monsalve, C. Mendoza-Buenrostro, S. Holmberg, N. A. Garza-Flores, M. A. Almajhadi, I. González-Gamboa, *Biofabrication* **2020**, *12*, 035023; d) E. J. Bolívar-Monsalve, C. F. Ceballos-González, C. Chávez-Madero, B. G. de la Cruz-Rivas, S. Velásquez Marín, S. Mora-Godínez, L. M. Reyes-Cortés, A. Khademhosseini, P. S. Weiss, M. Samandari, *Adv. Healthcare Mater.* **2022**, *11*, 2200448.
[37] Y. Cheng, Y. Yu, F. Fu, J. Wang, L. Shang, Z. Gu, Y. Zhao, *ACS. Appl. Mater.* **2016**, *8*, 1080.
[38] Y. Yu, F. Fu, L. Shang, Y. Cheng, Z. Gu, Y. Zhao, *Adv. Mater.* **2017**, *29*, 1605765.
[39] Y. Yu, W. Wei, Y. Wang, C. Xu, Y. Guo, J. Qin, *Adv. Mater.* **2016**, *28*, 6649.
[40] Y. Yu, H. Wen, J. Ma, S. Lykkemark, H. Xu, J. Qin, *Adv. Mater.* **2014**, *26*, 2494.
[41] a) P. Ghaderinejad, N. Najmoddin, Z. Bagher, M. Saeed, S. Karimi, S. Simorgh, M. Pezeshki-Modaress, *Chem. Eng. J.* **2021**, *420*, 130465; b) Y. Wang, L. Shang, Y. Zhao, L. Sun, *Engineering* **2022**, *13*, 128; c) Z. Wei, S. Wang, J. Hirvonen, H. A. Santos, W. Li, *Adv. Healthcare Mater.* **2022**, *11*, 2200846; d) B. Kong, R. Liu, J. Guo, L. Lu, Q. Zhou, Y. Zhao, *Bioact. Mater.* **2023**, *19*, 328.
[42] K. Braeckmans, S. C. De Smedt, C. Roelant, M. Leblans, R. Pauwels, J. Demeester, *Nat. Mater.* **2003**, *2*, 169.
[43] F. Fayazpour, B. Lucas, N. Huyghebaert, K. Braeckmans, S. Derveaux, B. G. Stubbe, J. P. Remon, J. Demeester, C. Vervaet, S. C. De Smedt, *Adv. Mater.* **2007**, *19*, 3854.
[44] a) D. C. Appleyard, S. C. Chapin, R. L. Srinivas, P. S. Doyle, *Nat. Protoc.* **2011**, *6*, 1761; b) S. E. Chung, W. Park, S. Shin, S. A. Lee, S. Kwon, *Nat. Mater.* **2008**, *7*, 581; c) Y. Xu, H. Wang, B. Chen, H. Liu, Y. Zhao, *Sci. China Mater.* **2018**, *62*, 289; d) S. Habasaki, W. C. Lee, S. Yoshida, S. Takeuchi, *Small* **2015**, *11*, 6391.
[45] a) H. J. M. Wolff, J. Linkhorst, T. Göttlich, J. Savinsky, A. J. D. Krüger, L. de Laporte, M. Wessling, *Lab Chip* **2020**, *20*, 285; b) M. A. Sahin, M. Shehzad, G. Destgeer, *Small* **2024**, *20*, 2307956.
[46] P. N. Manghnani, V. Di Francesco, C. Panella La Capria, M. Schlich, M. E. Miali, T. L. Moore, A. Zunino, M. Duocastella, P. Decuzzi, *J. Colloid Interface Sci.* **2022**, *608*, 622;
[47] H. Lee, J. Kim, H. Kim, J. Kim, S. Kwon, *Nat. Mater.* **2010**, *9*, 745.
[48] J. Lee, P. W. Bisso, R. L. Srinivas, J. J. Kim, A. J. Swiston, P. S. Doyle, *Nat. Mater.* **2014**, *13*, 524.
[49] J. Lolsberg, A. Cinar, D. Felder, G. Linz, S. Djeljadini, M. Wessling, *Small* **2019**, *15*, 1901356.
[50] A. K. Miri, D. Nieto, L. Iglesias, H. Goodarzi Hosseinabadi, S. Maharjan, G. U. Ruiz-Esparza, P. Khoshakhlagh, A. Manbachi, M. R. Dokmeci, S. Chen, S. R. Shin, Y. S. Zhang, A. Khademhosseini, *Adv. Mater.* **2018**, *30*, 1800242.
[51] a) Y. Liu, C. Shao, Y. Wang, L. Sun, Y. Zhao, *Matter* **2019**, *1*, 1581; b) S. H. Nam, J. Park, S. Jeon, *Adv. Funct. Mater.* **2019**, *29*, 1904971; c) M. Huang, Y. Wang, X. Liu, S. Zhang, C. L. Yuan, H. L. Hu, Z. G. Zheng, *Adv. Opt. Mater.* **2023**, *11*, 2300573.
[52] H. Kim, J. Ge, J. Kim, S.-e. Choi, H. Lee, H. Lee, W. Park, Y. Yin, S. Kwon, *Nat. Photonics* **2009**, *3*, 534.
[53] J. Li, D. Liang, X. Chen, W. Sun, X. Shen, *Biomed. Technol.* **2024**, *5*, 1.
[54] Y. Huo, Y. Xu, X. Wu, E. Gao, A. Zhan, Y. Chen, Y. Zhang, Y. Hua, W. Swieszkowski, Y. S. Zhang, *Adv. Sci.* **2022**, *9*, 2202181.
[55] a) M. N. S. I. K. Akita, *J. Imaging Sci. Technol.* **2008**, *52*, 060201; b) Y. Luo, A. Lode, M. Gelinsky, *Adv. Healthcare Mater.* **2013**, *2*, 777; c) T. Xu, W. Zhao, J. M. Zhu, M. Z. Albanna, J. J. Yoo, A. Atala, *Biomaterials* **2013**, *34*, 130; d) J. Gong, C. C. L. Schuurmans, A. M. V. Genderen, X. Cao, W. Li, F. Cheng, J. J. He, A. Lopez, V. Huerta, J. Manriquez, R. Li, H. Li, C. Delavaux, S. Sebastian, P. E. Capendale, H. Wang, J. Xie, M. Yu, R. Masereeuw, T. Vermonden, Y. S. Zhang, *Nat. Commun.* **2020**, *11*, 1267; e) R. Zimmermann, C. Hentschel, F.

Schron, D. Moedder, T. Buttner, P. Atallah, T. Wegener, T. Gehring, S. Howitz, U. Freudenberg, C. Werner, *Biofabrication* **2019**, *11*, 045008.
[56] W. Liu, Y. S. Zhang, M. A. Heinrich, F. De Ferrari, H. L. Jang, S. M. Bakht, M. M. Alvarez, J. Yang, Y. C. Li, G. Trujillo-de Santiago, A. K. Miri, K. Zhu, P. Khoshakhlagh, G. Prakash, H. Cheng, X. Guan, Z. Zhong, J. Ju, G. H. Zhu, X. Jin, S. R. Shin, M. R. Dokmeci, A. Khademhosseini, *Adv. Mater.* **2017**, *29*, 1604630.
[57] M. A. Skylar-Scott, J. Mueller, C. W. Visser, J. A. Lewis, *Nature* **2019**, *575*, 330.
[58] C. Yu, J. Schimelman, P. R. Wang, K. L. Miller, X. Y. Ma, S. T. You, J. A. Guan, B. J. Sun, W. Zhu, S. C. Chen, *Chem. Rev.* **2020**, *120*, 10695.
[59] a) K. Yu, X. J. Zhang, Y. Sun, Q. Gao, J. Z. Fu, X. J. Cai, Y. He, *Bioact. Mater.* **2022**, *11*, 254; b) Y. Yang, X. Song, X. Li, Z. Chen, C. Zhou, Q. Zhou, Y. Chen, *Adv. Mater.* **2018**, *30*, 1706539; c) M. Obst, T. Heinze, *Macromol. Mater. Eng.* **2016**, *301*, 65.
[60] X. Ma, X. Qu, W. Zhu, Y.-S. Li, S. Yuan, H. Zhang, J. Liu, P. Wang, C. S. E. Lai, F. Zanella, S. Chien, S. Chen, *Proc. Natl. Acad. Sci. USA* **2016**, *113*, 2206.
[61] F. Mayer, S. Richter, J. Westhauser, E. Blasco, C. Barner-Kowollik, M. Wegener, *Sci. Adv.* **2019**, *5*, 9160.
[62] a) J. Tang, R. Schutzman, C. A. Rodríguez, J. Lahann, N. Rodríguez-Hornedo, M. R. Prausnitz, S. P. Schwendeman, *J. Controlled Release* **2022**, *341*, 634; b) P. K. Baumgarten, *J. Colloid Interface Sci.* **1971**, *36*, 71; c) M. Bognitzki, W. Czado, T. Frese, A. Schaper, M. Hellwig, M. Steinhart, A. Greiner, J. H. Wendorff, *Adv. Mater.* **2001**, *13*, 70; d) Z. Guo, G. Tang, Y. Zhou, L. Shuwu, H. Hou, Z. Chen, J. Chen, C. Hu, F. Wang, S. C. De Smedt, R. Xiong, C. Huang, *Carbohydr. Polym.* **2017**, *169*, 198.
[63] a) M. C. George, P. V. Braun, *Angew. Chem., Int. Ed.* **2009**, *48*, 8606; b) J. Tian, Q. Ma, W. Yu, D. Li, X. Dong, G. Liu, J. Wang, *Mater. Des.* **2019**, *170*, 107701; c) K. J. Lee, T. H. Park, S. Hwang, J. Yoon, J. Lahann, *Langmuir* **2013**, *29*, 6181.
[64] S. Bhaskar, J. Lahann, *J. Am. Chem. Soc.* **2009**, *131*, 6650.
[65] C. Huang, B. Lucas, C. Vervaet, K. Braeckmans, S. Van Calenbergh, I. Karalic, M. Vandewoestyne, D. Deforce, J. Demeester, S. C. De Smedt, *Adv. Mater.* **2010**, *22*, 2657.
[66] S. Bhaskar, J. Hitt, S. W. Chang, J. Lahann, *Angew. Chem., Int. Ed. Engl.* **2009**, *48*, 4589.
[67] J. Yoon, T. W. Eyster, A. C. Misra, J. Lahann, *Adv. Mater.* **2015**, *27*, 4509.
[68] A. C. Misra, S. Bhaskar, N. Clay, J. Lahann, *Adv. Mater.* **2012**, *24*, 3850.
[69] K. J. Lee, J. Yoon, S. Rahmani, S. Hwang, S. Bhaskar, S. Mitragotri, J. Lahann, *Proc. Natl. Acad. Sci. USA* **2012**, *109*, 16057.
[70] a) S. Rahmani, S. Saha, H. Durmaz, A. Donini, A. C. Misra, J. Yoon, J. Lahann, *Angew. Chem., Int. Ed. Engl.* **2014**, *53*, 2332; b) J. Xue, C. Zhu, J. Li, H. Li, Y. Xia, *Adv. Funct. Mater.* **2018**, *28*, 1705563;
[71] K. H. Roh, D. C. Martin, J. Lahann, *J. Am. Chem. Soc.* **2006**, *128*, 6796.
[72] S. Haeberle, R. Zengerle, J. Ducrée, *Microfluid. Nanofluid.* **2006**, *3*, 65.
[73] M. Hayakawa, H. Onoe, K. H. Nagai, M. Takinoue, *Sci. Rep.* **2016**, *6*, 20793.
[74] a) Q. Qu, W. Cheng, X. Zhang, A. Zhou, Y. Deng, M. Zhu, T. Chu, B. B. Manshian, R. Xiong, S. J. Soenen, *Biomacromolecules* **2022**, *23*, 3572; b) Q. Qu, X. Zhang, A. Yang, J. Wang, W. Cheng, A. Zhou, Y. Deng, R. Xiong, C. Huang, *J. Colloid Interface Sci.* **2022**, *626*, 768; c) Z. C. Ding, Z. M. Liang, X. Rong, X. X. Fu, J. X. Fan, Y. H. Lai, Y. R. Cai, C. Huang, L. L. Li, G. S. Tang, Z. Y. Luo, Z. K. Zhou, *Small* **2024**, *20*, 2403753.
[75] A. V. Anilkumar, I. Lacik, T. G. Wang, *Biotechnol. Bioeng.* **2001**, *75*, 581.
[76] a) X. Zhang, Q. Qu, W. Cheng, A. Zhou, Y. Deng, W. Ma, M. Zhu, R. Xiong, C. Huang, *Int. J. Biol. Macromol.* **2022**, *209*, 794; b) V. Pal, Y. P. Singh, D. Gupta, M. A. Alioglu, M. Nagamine, M. H. Kim, I. T. Ozbolat, *Biofabrication* **2023**, *15*, 035001; c) H. Liu, Z. Cai, F. Wang, L. Hong, L. Deng, J. Zhong, Z. Wang, W. Cui, *Adv. Sci.* **2021**, *8*, 2101619; d) R. Ghaffarian, E. Pérez-Herrero, H. Oh, S. R. Raghavan, S. Muro, *Adv. Funct. Mater.* **2016**, *26*, 3382.
[77] G. Tang, R. Xiong, D. Lv, R. X. Xu, K. Braeckmans, C. Huang, S. C. De Smedt, *Adv. Sci.* **2019**, *6*, 1802342.
[78] G. Tang, L. Chen, Z. Wang, S. Gao, Q. Qu, R. Xiong, K. Braeckmans, S. C. De Smedt, Y. S. Zhang, C. Huang, *Small* **2020**, *16*, 1907586.
[79] A. Choi, K. D. Seo, B. C. Kim, D. S. Kim, *Lab Chip* **2017**, *17*, 591.
[80] C. H. Choi, B. Lee, J. Kim, J. O. Nam, H. Yi, C. S. Lee, *ACS. Appl. Mater. Interfaces* **2015**, *7*, 11393.
[81] a) W. Gao, A. Pei, R. Dong, J. Wang, *J. Am. Chem. Soc.* **2014**, *136*, 2276; b) Y. Wu, T. Si, J. Shao, Z. Wu, Q. He, *Nano Res.* **2016**, *9*, 3747.
[82] J. Shao, M. Abdelghani, G. Shen, S. Cao, D. S. Williams, J. C. M. van Hest, *ACS Nano* **2018**, *12*, 4877.
[83] R. Luo, Y. Cao, P. Shi, C. H. Chen, *Small* **2014**, *10*, 4886.
[84] M. Y. Chiang, Y. W. Hsu, H. Y. Hsieh, S. Y. Chen, S. K. Fan, *Sci. Adv.* **2016**, *2*, 1600964.
[85] K. Cho, H. J. Lee, S. W. Han, J. H. Min, H. Park, W. G. Koh, *Angew. Chem., Int. Ed. Engl.* **2015**, *54*, 11511.
[86] a) K. O. Rojek, M. Ćwiklińska, J. Kuczak, J. Guzowski, *Chem. Rev.* **2022**, *122*, 16839; b) C. M. Shao, J. J. Chi, L. R. Shang, Q. H. Fan, F. F. Ye, *Acta Biomater.* **2022**, *138*, 21.
[87] a) D. Ribezzi, M. Gueye, S. Florczak, F. Dusi, D. de Vos, F. Manente, A. Hierholzer, M. Fussenegger, M. Caiazzo, T. Blunk, J. Malda, R. Levato, *Adv. Mater.* **2023**, *35*, 2301673; b) Y. Qian, J. X. Gong, K. J. Lu, Y. Hong, Z. Y. Zhu, J. Y. Zhang, Y. W. Zou, F. F. Zhou, C. Y. Zhang, S. Y. Zhou, T. Y. Gu, M. Sun, S. L. Wang, J. X. He, Y. Li, J. X. Lin, Y. Yuan, H. W. Ouyang, M. F. Yu, H. M. Wang, *Biomaterials* **2023**, *299*, 122137; c) C. Chavez-Madero, M. Diaz de Leon-Derby, M. Samandari, C. F. Ceballos-Gonzalez, E. J. Bolivar-Monsalve, C. C. Mendoza-Buenrostro, S. Holmberg, N. A. Garza-Flores, M. A. Almajhadi, I. Gonzalez-Gamboa, J. F. Yee-de Leon, S. O. Martinez-Chapa, C. A. Rodriguez, H. K. Wickramasinghe, M. J. Madou, D. Dean, A. Khademhosseini, Y. S. Zhang, M. M. Alvarez, G. Trujillo de Santiago, *Biofabrication* **2020**, *12*, 035023.
[88] a) L. Yang, Y. X. Liu, L. Y. Sun, C. Zhao, G. P. Chen, Y. J. Zhao, *Nano-Micro Lett.* **2022**, *14*, 4; b) Y. Huang, M. Zhan, H. Sun, C. Zhang, M. Shen, J. Ma, G. Zhang, X. Shi, *J. Colloid Interface Sci.* **2025**, *686*, 498.
[89] a) J. B. Li, Y. T. Wang, L. J. Cai, L. R. Shang, Y. J. Zhao, *Chem. Eng. J.* **2022**, *427*, 130750; b) T. Kubota, Y. Kurashina, J. Y. Zhao, K. Ando, H. Onoe, *Mater. Des.* **2021**, *203*, 109580.
[90] a) Z. N. Wu, Y. J. Zheng, J. M. Lin, Y. X. Li, Y. N. Lin, X. R. Wang, L. Lin, *Chem. Eng. J.* **2024**, *481*, 148403; b) Q. L. Qu, X. L. Zhang, H. Ravanbakhsh, G. S. Tang, J. Zhang, Y. K. Deng, K. Braeckmans, S. C. De Smedt, R. H. Xiong, C. B. Huang, *Chem. Eng. J.* **2022**, *428*, 132607.
[91] R. Garg, S. Gonuguntla, S. Sk, M. S. Iqbal, A. O. Dada, U. Pal, M. Ahmadipour, *Adv. Colloid Interface Sci.* **2024**, *330*, 103203.
[92] a) F. He, M. J. Zhang, W. Wang, Q. W. Cai, Y. Y. Su, Z. Liu, Y. Faraj, X. J. Ju, R. Xie, L. Y. Chu, *Adv. Mater. Technol.* **2019**, *4*, 1800687; b) J. Qin, Z. Li, B. Song, *J. Mater. Chem. B* **2020**, *8*, 1682.
[93] Y. Liu, L. Sun, H. Zhang, L. Shang, Y. Zhao, *Chem. Rev.* **2021**, *121*, 7468.
[94] J. Mu, D. Luo, W. Li, Y. Ding, *Biomed. Technol.* **2024**, *5*, 60.
[95] X. Zhang, Q. Qu, A. Zhou, Y. Wang, J. Zhang, R. Xiong, V. Lenders, B. B. Manshian, D. Hua, S. J. Soenen, *Adv. Colloid Interface Sci.* **2022**, *299*, 102568.

[96] X.-T. Sun, R. Guo, D.-N. Wang, Y.-Y. Wei, C.-G. Yang, Z.-R. Xu, *J. Colloid Interface Sci.* **2019**, *553*, 631.
[97] J. V. Weaver, S. P. Rannard, A. I. Cooper, *Angew. Chem., Int. Ed. Engl.* **2009**, *48*, 2131.
[98] B. H. Shan, F. G. Wu, *Adv. Mater.* **2024**, *36*, 2210707.
[99] F. He, W. Wang, X.-H. He, X.-L. Yang, M. Li, R. Xie, X.-J. Ju, Z. Liu, L.-Y. Chu, *ACS. Appl. Mater. Interfaces* **2016**, *8*, 8743.
[100] H. U. Kim, D. G. Choi, Y. H. Roh, M. S. Shim, K. W. Bong, *Small* **2016**, *12*, 3463.
[101] Y. Yu, G. Chen, J. Guo, Y. Liu, J. Ren, T. Kong, Y. Zhao, *Mater. Horiz.* **2018**, *5*, 1137.
[102] a) H. Wang, X.-Y. You, G.-P. Zhao, *Sci. Bull.* **2025**, *70*, 305; b) L. Nuhn, *Nat. Nanotechnol.* **2023**, *18*, 550; c) S. He, L. G. Leanse, Y. Feng, *Adv. Drug Delivery Rev.* **2021**, *178*, 113922.
[103] S. P. M. Sriram, A. Mahajan, D. S. Katti, *Biofabrication* **2024**, *16*, 1758.
[104] Y.-C. Lu, W. Song, D. An, B. J. Kim, R. Schwartz, M. Wu, M. Ma, *J. Mater. Chem. B* **2015**, *3*, 353.
[105] Q. Wu, C. Yang, G. Liu, W. Xu, Z. Zhu, T. Si, R. X. Xu, *Lab Chip* **2017**, *17*, 3168.
[106] Z. Wu, Y. Zheng, L. Lin, S. Mao, Z. Li, J. M. Lin, *Angew. Chem., Int. Ed. Engl.* **2020**, *59*, 2225.
[107] B. Y. Liu, Q. L. Liu, J. C. Feng, *Adv. Mater.* **2024**, *36*, 2404977.
[108] Z. Zhao, H. Wang, L. Shang, Y. Yu, F. Fu, Y. Zhao, Z. Gu, *Adv. Mater.* **2017**, *29*, 1704569.
[109] Y. Liu, L. Shang, H. Wang, H. Zhang, M. Zou, Y. Zhao, *Mater. Horiz.* **2018**, *5*, 979.
[110] G. Tang, L. Chen, Z. Wang, S. Gao, C. Huang, *Small* **2020**, *16*, 1907586.
[111] L.-H. Fu, C. Qi, T. Sun, K. Huang, J. Lin, P. Huang, *Exploration* **2023**, *3*, 20210110.
[112] a) J. Shi, Y. Wu, S. Zhang, Y. Tian, D. Yang, Z. Jiang, *Chem. Soc. Rev.* **2018**, *47*, 4295; b) Y. Chen, M. Yuan, Y. Zhang, S. Liu, X. Yang, K. Wang, J. Liu, *Chem. Sci.* **2020**, *11*, 8617.
[113] a) B. Stadler, R. Chandrawati, A. D. Price, S. F. Chong, K. Breheney, A. Postma, L. A. Connal, A. N. Zelikin, F. Caruso, *Angew. Chem., Int. Ed. Engl.* **2009**, *48*, 4359; b) Y. Elani, R. V. Law, O. Ces, *Nat. Commun.* **2014**, *5*, 5305; c) M. E. Allen, J. W. Hindley, D. K. Baxani, O. Ces, Y. Elani, *Nat. Rev. Chem.* **2022**, *6*, 562.
[114] a) S. C. Shetty, N. Yandrapalli, K. Pinkwart, D. Krafft, T. Vidakovic-Koch, I. Ivanov, T. Robinson, *ACS Nano* **2021**, *15*, 15656; b) J.-W. Kim, S. H. Han, Y. H. Choi, W. M. Hamonangan, Y. Oh, S.-H. Kim, *Lab Chip* **2022**, *22*, 2259; c) Z. Chen, S. Kheiri, E. W. Young, E. Kumacheva, *Langmuir* **2022**, *38*, 6233; d) C. Martino, A. J. deMello, *Interface Focus* **2016**, *6*, 20160011.
[115] H. Wang, Z. Zhao, Y. Liu, C. Shao, F. Bian, Y. Zhao, *Sci. Adv.* **2018**, *4*, 2816.
[116] Q. Qu, X. Zhang, H. Ravanbakhsh, G. Tang, J. Zhang, Y. Deng, K. Braeckmans, S. C. De Smedt, R. Xiong, C. Huang, *Chem. Eng. J.* **2022**, *428*, 132607.
[117] a) W. Gao, X. Feng, A. Pei, Y. Gu, J. Li, J. Wang, *Nanoscale* **2013**, *5*, 4696; b) Z. Lin, C. Gao, D. Wang, Q. He, *Angew. Chem., Int. Ed. Engl.* **2021**, *60*, 8750.
[118] a) R. Maria-Hormigos, B. Jurado-Sánchez, A. Escarpa, *Anal. Bioanal. Chem.* **2022**, *414*, 7035; b) Q. Wang, C. Wang, X. Yang, J. Wang, Z. Zhang, L. Shang, *Smart Med.* **2023**, *2*, 20220027.
[119] a) B. E.-F. de Ávila, P. Angsantikul, J. Li, M. A. Lopez-Ramirez, D. E. Ramírez-Herrera, S. Thamphiwatana, C. Chen, J. Delezuk, R. Samakapiruk, V. Ramez, *Nat. Commun.* **2017**, *8*, 272; b) S. K. Srivastava, G. Clergeaud, T. L. Andresen, A. Boisen, *Adv. Drug Delivery Rev.* **2019**, *138*, 41; c) H. Choi, S. H. Jeong, T. Y. Kim, J. Yi, S. K. Hahn, *Bioact. Mater.* **2022**, *9*, 54; d) F. Zhang, Z. Li, Y. Duan, A. Abbas, R. Mundaca-Uribe, L. Yin, H. Luan, W. Gao, R. H. Fang, L. Zhang, *Sci. Rob.* **2022**, *7*, 4160.
[120] a) Y. Yoshizumi, K. Okubo, M. Yokokawa, H. Suzuki, *Langmuir* **2016**, *32*, 9381; b) W. Chen, H. Zhou, B. Zhang, Q. Cao, B. Wang, X. Ma, *Adv. Funct. Mater.* **2022**, *32*, 2110625.
[121] L. Cai, D. Xu, H. Chen, L. Wang, Y. Zhao, *Eng. Regener.* **2021**, *2*, 109.
[122] B. Jurado-Sanchez, S. Sattayasamitsathit, W. Gao, L. Santos, Y. Fedorak, V. V. Singh, J. Orozco, M. Galarnyk, J. Wang, *Small* **2015**, *11*, 499.
[123] V. V. Singh, B. Jurado-Sánchez, S. Sattayasamitsathit, J. Orozco, J. Li, M. Galarnyk, Y. Fedorak, J. Wang, *Adv. Funct. Mater.* **2015**, *25*, 2147.
[124] G. Tang, L. Chen, L. Lian, F. Li, H. Ravanbakhsh, M. Wang, Y. S. Zhang, C. Huang, *Chem. Eng. J.* **2021**, *407*, 127187.
[125] L. Cai, H. Wang, Y. Yu, F. Bian, Y. Wang, K. Shi, F. Ye, Y. Zhao, *Natl. Sci. Rev.* **2020**, *7*, 644.
[126] L. Cai, C. Zhao, H. Chen, L. Fan, Y. Zhao, X. Qian, R. Chai, *Adv. Sci.* **2022**, *9*, 2103384.
[127] X. T. Sun, Y. Zhang, D. H. Zheng, S. Yue, C. G. Yang, Z. R. Xu, *Biosens. Bioelectron.* **2017**, *92*, 81.
[128] L. Sanchez, Y. Yi, Y. Yu, *Nanoscale* **2017**, *9*, 288.
[129] W. Li, J. Yan, Y. Yu, *Proc. Natl. Acad. Sci. USA* **2019**, *116*, 25106.

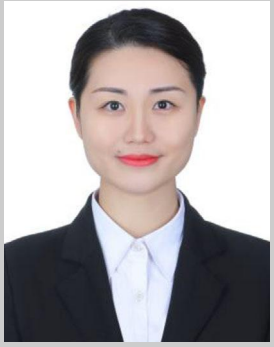

Yingying Hou received her B.S. and Master's degrees from Jilin Agricultural University (2013 and 2016). She is currently a Ph.D. candidate in the School of Biomedical Engineering at Guangzhou Medical University. Her research centers on novel bioink development, all aqueous biofabrication, and 3D bioprinting.

Leyan Xuan received her B.S. degree from Guangdong Medical University in 2022. She is pursuing her M.S. degree in pharmacy at Guangzhou Medical University. Her research focuses on 3D bioprinting, single-cell encapsulation, and cell delivery for regenerative medicine.

Weihong Mo is an undergraduate clinical pharmacy student at Guangzhou Medical University. Her research focuses on 3D bioprinting and fabricating biomimetic gradient porous architectures.

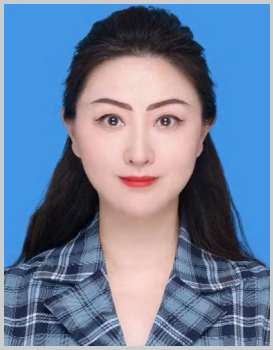

Yuanye Dang, Ph.D. in biomedical sciences from the University of Macau, postdoctoral fellow at the University of Kentucky in the United States, currently serves as an associate professor and Master's supervisor at Guangzhou Medical University. Her main research interests focus on pharmacology and efficacy of natural products, as well as research on new drug carriers.

Maobin Xie received his Ph.D. degree of biomedical engineering from The Hong Kong Polytechnic University, Hong Kong, China, and then works as postdoctoral research fellow at Harvard University, Boston, USA. He is now a professor at Guangzhou Medical University, Guangzhou, China. His research interests include volumetric 3D (bio)printing and biomaterials.

Guosheng Tang received his B.S. and Master's degrees from Jilin Agricultural University and a Ph.D. at Nanjing Forestry University. He worked with Prof. Y. Shrike Zhang at Harvard Medical School as a joint Ph.D. candidate and postdoctoral research fellow from 2019 to 2021. He is currently a professor at Guangzhou Medical University. His research is focused on innovating medical engineering technologies, including 3D bioprinting, gas-shearing-based microfluidics, and all aqueous biofabrication, to fabricate microgels or microgel assembly to recreate functional tissues and their biomimetic models for applications in tissue engineering and regenerative medicine.